BOREAS An international journal of Quaternary research

Aquatic and terrestrial proxy evidence for Middle Pleistocene palaeolake and lake-shore development at two Lower Palaeolithic sites of Schöningen, Germany

KIM J. KRAHN, MARIO TUCCI, BRIGITTE URBAN, JULIEN PILGRIM, PETER FRENZEL, INGEBORG SOULIÉ-MÄRSCHE AND ANTJE SCHWALB

BOREAS

Krahn, K. J., Tucci, M., Urban, B., Pilgrim, J., Frenzel, P., Soulié-Märsche, I. & Schwalb, A.: Aquatic and terrestrial proxy evidence for Middle Pleistocene palaeolake and lake-shore development at two Lower Palaeolithic sites of Schöningen, Germany. *Boreas*. https://doi.org/10.1111/bor.12523. ISSN 0300-9483.

The archaeological sites in the open-cast mine of Schöningen, Germany, represent outstanding archives for understanding Middle Pleistocene interglacial–glacial transitions and human adaption. Aquatic microfossil and pollen assemblages from the 'Reinsdorf sequence', likely correlated to Marine Isotope Stage 9, document environmental changes from a thermal maximum to succeeding glacial conditions recorded in two sequences of excavation sites 12 II and 13 II. Multi-proxy analyses enable detailed reconstruction of lake-shore and landscape developments despite variable microfossil preservation in changing carbonate- and organic-rich deposits. Rich aquatic vegetation with abundant charophytes suggests repeated phases with water depths of 0.5–2 m at site 13 II, while even greater temporary depths are deduced for 12 II DB. Mesorheophilic and mesotitanophilic ostracod species indicate stream inflows with medium–low calcium contents of >18 mg Ca L^{-1} originating from nearby springs. Diatoms point to meso-eutrophic conditions and an alkaline pH of the lake water. Interglacial conditions with thermophile forests but no aquatic microfossils preserved, suggesting a dry or only temporarily flooded site, mark the beginning of the sequence. Continuous presence of aquatic organisms and overall dominance of small tychoplanktonic diatoms during a subsequent cool steppe phase provide evidence for increased water depths and unstable habitats characterized by erosion and probably prolonged periods of lake ice cover. During the succeeding boreal forest-steppe phase, surface runoff into the productive, shallow lake decreased due to a more extensive vegetation cover. Concurrently, intensified groundwater input in contact with the nearby salt wall caused elevated salinities. Following a lake level drop, stream inflows and lake levels increased again towards the end of the Reinsdorf sequence and promoted development of a diverse fauna and flora at the lake shore; thereby maintaining an attractive living and hunting environment for early humans during a phase of generally cooler temperatures and landscape instability at the transition into a glacial period.

Kim J. Krahn (k.krahn@tu-braunschweig.de), Julien Pilgrim and Antje Schwalb, Institute of Geosystems and Bioindication, Technische Universität Braunschweig, Langer Kamp 19c, Braunschweig 38106, Germany; Mario Tucci and Brigitte Urban, Institute of Ecology, Landscape Change, Leuphana University Lüneburg, Universitätsallee 1, Lüneburg 21335, Germany; Peter Frenzel, Institute of Geosciences, Friedrich Schiller University Jena, Burgweg 11, Jena 07749, Germany; Ingeborg Soulié-Märsche, Institut des Sciences de l'Évolution (ISE-M), Université de Montpellier – CNRS, Case 061, Place Eugène Bataillon, Montpellier 34095, France; *received 4th October 2020, accepted 27th February 2021.*

The deposits in the open-cast lignite mine of Schöningen, eastern Lower Saxony, Germany, contain one of the most important Lower Palaeolithic sites that is internationally renowned for the worldwide oldest wooden hunting spears associated with diverse floral and faunal remains and flint artifacts (e.g. Thieme 2007; van Kolfschoten 2014; Serangeli *et al.* 2015, 2018). These finds prove hitherto unknown organized hunting, complex abstract thinking, and cognitive abilities of *Homo heidelbergensis* (Conard *et al.* 2015). Environmental information at high resolution as well as the abundant artifacts (Thieme 2007) enable direct correlation of climatic change and human adaption. The well-preserved weapons were embedded in an exceptionally complete sequence of Middle Pleistocene sediments, deposited between Elsterian and Saalian glacial tills, during the locally named Reinsdorf Interglacial (Urban *et al.* 1991a; Urban 1995, 2007). Based on thermoluminescence dating of heated flint from stratigraphically underlying deposits (13 I) a correlation of the so-called 'Spear Horizon' with Marine Isotope Stage (MIS) 9 was proposed (Richter & Krbetschek 2015). A recently obtained age of about 300 ka of sediments from the Reinsdorf sequence, based on luminescence dating, supports this correlation (Tucci *et al.* 2021). Results thereby agree well with recent stratigraphical interpretations from central Europe allocating the Elsterian to MIS 12 and the Holsteinian to MIS 11 (Lauer & Weiss 2018).

Since 1981/1982, samples of Pleistocene deposits have been recovered and analysed for geo-, bio- and archaeological studies. Especially the palaeolake-shore excavation site 13 II, where in level 4 eight wooden hunting spears along with remains of more than 20 butchered horses and around 1500 stone artefacts were discovered, is of great interest for understanding human behaviour and evolution (Thieme 1997, 1999, 2007; Serangeli *et al.* 2012, 2018).

DOI 10.1111/bor.12523

Biological and geochemical proxies preserved in lake sediments have long been used to reconstruct large-scale to site-specific short-term climate variations as they can provide high-resolution palaeoenvironmental information (Last & Smol 2001; Smol *et al.* 2001a, b; Hoelzmann *et al.* 2010; Pérez *et al.* 2013). For example, aquatic microfossils such as ostracods and diatoms allow the reconstruction of past temperatures (Kumke *et al.* 2004; Horne *et al.* 2012), salinity and conductivity (Gasse *et al.* 1987; Reed *et al.* 2012; McCormack *et al.* 2019), water depths (Wrozyna *et al.* 2009) and trophic status (Smol & Stoermer 2010).

The goal of this paper is to draw a more consistent picture of Middle Pleistocene human habitats during the transition of the Reinsdorf Interglacial and succeeding forest and steppe phases into a glacial period by providing qualitative and quantitative environmental information from aquatic and terrestrial proxies. We use fossil ostracod, diatom and charophyte assemblages preserved in sediments of two archaeologically important sites (Schöningen 12 II, Schöningen 13 II) to document lake level, nutrient level and salinity changes and further reconstruct palaeolake-shore characteristics, such as stream inflow and water depth. Statistically refined palynological interpretations of data published by Urban & Bigga (2015) serve for comparison with vegetation development and provide the biostratigraphical framework.

Site description

The open-cast lignite mine of Schöningen (latitude 52°8′N, longitude 11°0′E, altitude 90–130 m a.s.l.) is located in eastern Lower Saxony, northern Germany, about 100 km east of Hanover (Fig. 1A) at the southeastern edge of the Muschelkalk limestone ridge of the Elm. The Stassfurt-Helmstedter salt wall, a 70-km-long narrow salt structure, runs in a northwest–southeast direction along the northeastern area of the mine (Brandes *et al.* 2012). Until 2008/2009 the pit was separated into a northern and a southern mining area by a dam (Deutsche-Bahn-Pfeiler, 'DB'; Fig. 1B).

A sequence of six superimposed interglacial–glacial cycles was identified in the mine. Mania (1995, 2007a) interpreted these deposits as infillings of northwest to southeast trending large-scale fluvial channels overlying Elsterian till, each one starting with late glacial sediments, discordantly overlain by silty, organic-rich limnic-telmatic sediments covering an interglacial and its transition into the succeeding glacial period. This interpretation provided the nomenclature of the individual sites ('channels I to VI'). However, based on data from outcrop sections, shear wave seismics and borehole logs, Lang *et al.* (2012, 2015) challenged this model and inferred deposition of the interglacial sequences within a shallow, elongated lake basin, formed in the depression of an Elsterian tunnel valley. A long-lived lake, infilled by delta sediments and fed by small streams from the Elm ridge, was proposed, and the 'channels' were interpreted to represent major unconformities within the palaeo-delta caused by climate-driven lake level changes. According to this view, sites 12 II and 13 II were located on a delta plain at the southwestern shore of the palaeolake.

Sandwiched between Elsterian and Saalian glacial deposits, three succeeding interglacial–glacial cycles were defined by Urban *et al.* (1988, 1991a, b) and Urban (1995) based on palynological evidence. The oldest interglacial deposits overlying Elsterian till from the northern mining area were assigned to the Holsteinian Interglacial ('channel I'). The mid- to late interglacial pollen succession from 'channel II' (southern mining area) differs considerably from these Holsteinian deposits and those from other Holsteinian sequences in northern Germany. Therefore, this succession was locally defined as the Reinsdorf Interglacial and later correlated with Marine Isotope Stage (MIS) 9 (Urban *et al.* 2011; Sierralta *et al.* 2012; Urban & Bigga 2015). The warm climatic period represented by 'channel III' deposits in the northern mining area was named the Schöningen Interglacial and based on biostratigraphical evidence and $^{230}U/^{234}Th$ dating correlated with MIS 7 (Urban *et al.* 1991a; Heijnis 1992; Urban 1995, 2007).

Material and methods

Sampling and lithological description

Reference Profile 13 II (2003). – At archaeological site 13 II (56°07′59″N, 10°59′19″E; Fig. 1C), a 10.25-m-thick sediment sequence was designated as Reference Profile (RP). It was lithologically described by Mania in Böhner *et al.* (2005) and Thieme (2007), and sedimentologically and geochemically investigated by Urban & Bigga (2015) (Table S1). Samples for palynological and geochemical analysis were taken at five staggered profiles (squares) in 2003 from RP 13 II (Urban & Bigga 2015; Fig. 1D). From these samples, subsamples were separated for aquatic microfossil (62 samples) and geochemical analyses (51 samples), each 1–2 cm thick. No material was left to analyse level 13 II-4b(c) 4a ('Spear Horizon'). The designation (13 = archaeological site, II = channel/climatic cycle) and subdivision (level: II-1 to 5, sublevel: e.g. II-1a, sub-sublevel: e.g. II-1a1) follows Mania (1998), Böhner *et al.* (2005) and Urban & Bigga (2015).

Ostracods, diatoms and charophytes were analysed at the Institute of Geosystems and Bioindication (IGeo), TU Braunschweig, geochemical analyses were prepared at IGeo and further carried out at the GFZ German Research Centre for Geosciences, Potsdam. Palynological analyses were performed in the Laboratory of Palynology, Institute of Ecology, Leuphana University of Lüneburg.

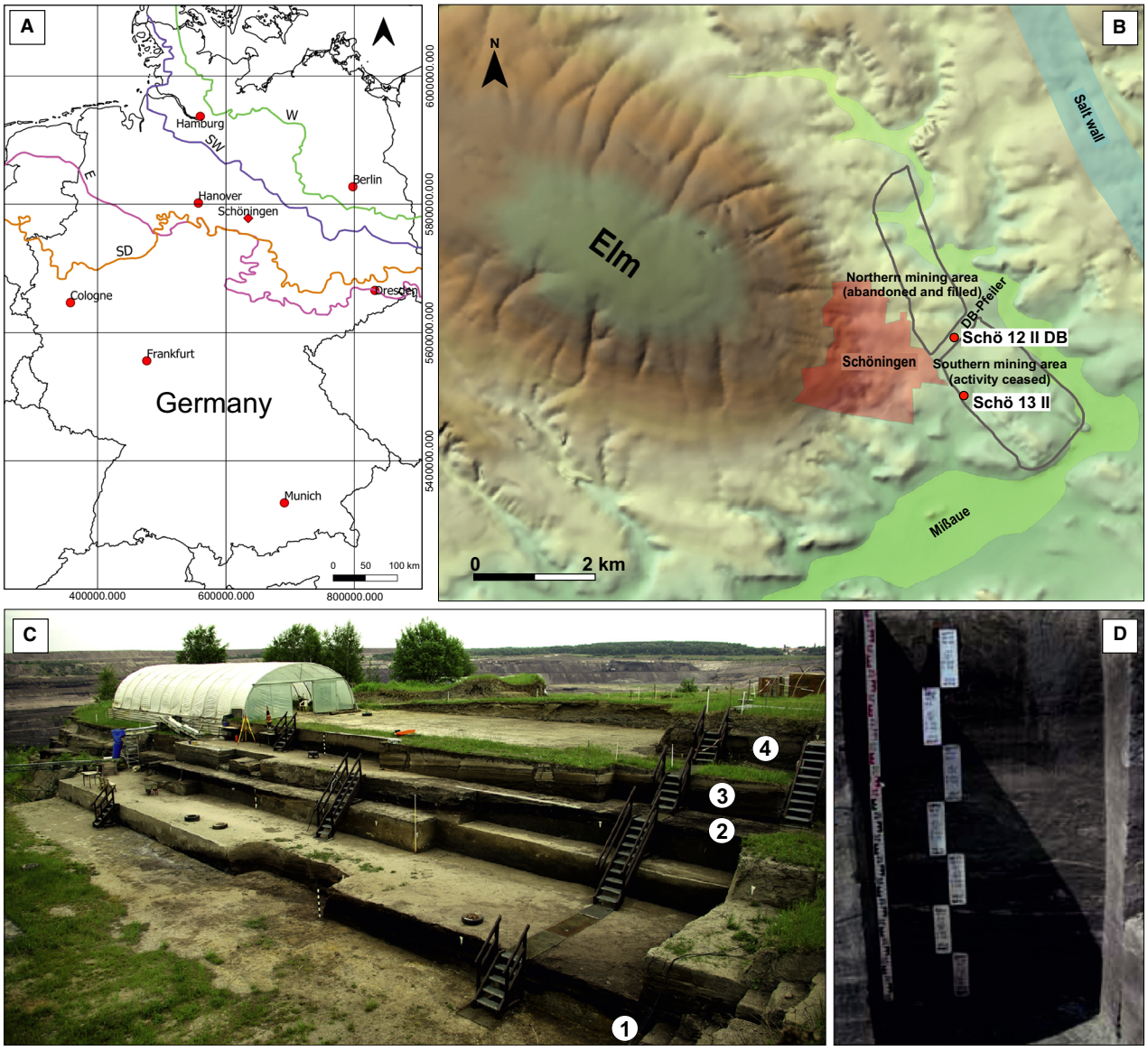

Fig. 1. A. Location of Schöningen (red rhombus) in Germany and maximum extent of Pleistocene ice sheets (coloured lines; E = Elsterian; SW = Saalian Warthe ice advance; SD = Saalian Drenthe ice advance; W = Weichselian; modified from Tucci *et al.* 2021). B. Digital elevation model showing the Elm, Schöningen, position of the open-cast mine with archaeological sites (Schöningen 13 II, 12 II DB), salt wall covered by Palaeogene sediments (position from Brandes *et al.* 2012) and the modern Mißaue flood-plain (modified from Serangeli *et al.* 2018; original map by U. Böhner, NLD, Hanover; DEM by D. Fabian). C. Archaeological site Schöningen 13 II with levels 1–4 of terrestrial and lacustrine sediments corresponding to the Reference Profile Schöningen 13 II (2003) (photograph: J. Serangeli 2012). D. Example of continuous profile sampling at profile Schöningen 12 II x-897, y579 (2009) (photograph: J. Serangeli).

Profile Schöningen 12 II DB (2009). – During the excavation of the 'DB-Pfeiler' prior to mining the underlying brown coal seams, site Schöningen 12 II as well as under- and overlying sediments were exposed, excavated and described (Lang & Winsemann 2012; Lang *et al.* 2012; Serangeli *et al.* 2012; Kunz *et al.* 2017; Table S2). Excavations were conducted stepwise on plateaus.

Samples of the sedimentary sequence 12 II DB (2009) were collected for palynological and geochemical analysis at plateau 4 from four staggered profiles: Schöningen 12 II x-897, y579 (2009) (52°8'32.37"N, 10°59'12.99"E; Fig. 1D), Schöningen 12 II x903, y598 (2009) (52°8';32.67"N, 10°59'13.87"E), Schöningen 12 II x-899, y615 (2009) (52°8'33.16"N, 10°59'14.39"E) and Schöningen 12 II x-896, y603.4 (2009) (52°8'32.96"N, 10°59'13.82"E) (Julien *et al.* 2015; Kunz *et al.* 2017; Table S2; Fig. 1D). Subsamples for aquatic microfossil and geochemical analyses were later taken from these palynological samples. Except for two samples, which

had to be merged with samples from adjoining depths to have sufficient sediment for analysis, subsamples were 1–2 cm thick.

Ostracod and charophyte analysis

A total of 60 and 42 samples, respectively, were analysed for ostracods and charophyte gyrogonites in RP 13 II (2003) and 12 II DB (2009). Between 3 and 8 g (RP 13 II) and 5–10 g (12 II DB) sediment was processed. For one sample of the RP (RP56), only 1 g was available. Samples were immersed overnight in ~4% H_2O_2 to disaggregate the sediment and then washed through stacked 250-, 125- and 63-µm mesh sieves. If possible, 300 valves were extracted from the 250-µm fraction with fine brushes and identified using a Leica M80 stereoscopic microscope. Because of the limited amount of sediment and partially poor preservation, a sufficient valve number was only reached in seven samples of RP 13 II. In sequence 12 II DB (2009), the 250-µm fraction provided constantly fewer than 300 ostracods. Samples with fewer than 10 identified ostracod valves (RP 13 II: three samples, 12 II DB: one sample) were excluded from the quantitative reconstructions. Valves in the smaller fractions were counted to assess the ostracod concentration (valves per gram dry weight). Whole carapaces were counted as two valves. The 63-µm fraction samples of 12 II DB (2009) were analysed using two defined crossing transect lines and count numbers extrapolated. Intact adult and juvenile ostracod valves and valve fragments were counted separately to assess adult/juvenile-ratio and preservation. Taxonomic identification of ostracods was carried out using standard identification keys (e.g. Meisch 2000; Fuhrmann 2012). Additionally, gyrogonites of charophytes were separated from the same samples, counted and identified. The identification is based on Soulié-Märsche (1989), Détriché *et al.* (2009), Soulié-Märsche & García (2015), and Sanjuan *et al.* (2017). Only samples with more than five identified gyrogonites were used for quantitative reconstructions.

Diatom analysis

For diatoms, 59 (RP 13 II) and 39 (12 II DB) samples were analysed. Preparation of samples was performed after Kalbe & Werner (1974) with minor modifications. Naphrax® was used as mountant to prepare permanent slides for light microscope analyses. Diatom counting was performed using a Leica DM 5000 B LM equipped with a ProgRes® CT5 camera with differential interference contrast under oil immersion at ×1000 magnification. Diatom concentration was determined by adding known quantities of microspheres (Battarbee & Kneen 1982) and valves were identified using standard literature (e.g. Krammer & Lange-Bertalot 1986, Krammer & Lange-Bertalot 1998, 1991a, b; Lange-Bertalot *et al.* 2017) and relevant taxonomic publications. If possible, 400 valves per sample were identified. Analysis of samples of RP 13 II (2003) lacking diatoms or with extremely low diatom concentration was stopped when 500 microspheres and fewer than 10 diatom valves had been counted. In samples with low diatom concentration, valves were counted until 1000 microspheres had been reached. Samples containing fewer than 25 identified diatom valves were excluded from the quantitative reconstruction. In sequence 12 II DB (2009), analyses were stopped when 1000 microspheres had been counted.

Palynological analyses

Approximately 10 g of each sample was treated by standard palynological methods (Faegri & Iversen 1989; Moore *et al.* 1991). Details for sample selection and preparation for palynological analyses of RP 13 II (2003) and 12 II DB (2009) can be found in Urban & Bigga (2015) and Kunz *et al.* (2017), respectively.

Analysis of TOC, TN, $CaCO_3$ and C/N

In total, 51 samples of RP 13 II (2003) and 35 samples of sequence 12 II DB (2009) were analysed for total nitrogen (TN), total organic carbon (TOC), total carbon (TC) and $CaCO_3$ for further aquatic microfossil sample correlated information in addition to the already established geochemical data. For TC and TN, around 10 mg of sample material was loaded in tin capsules. The TC and TN contents were calibrated against acetanilide and verified with a soil reference sample (Boden3, HEKA-TECH). For TOC determination the samples were prepared by *in-situ* decalcification. Around 3 mg of sample material was weighed into Ag-capsules and treated with 3% and then with 20% HCl solution droplets repeatedly until complete removal of carbonates. Subsequently, the samples were heated for 3 h at 75 °C and finally wrapped and measured. TC, TOC and TN were determined using an elemental analyser (ISOLINK EA) coupled with a ConFloIV interface on a DELTA V Advantage isotope ratio mass spectrometer (Thermo Fischer Scientific). The reproducibility for replicate analyses was 0.2% for TC, TN and TOC. The atomic C/N ratio is based on the TOC and TN mass relationship. The $CaCO_3$ content was calculated using the equation $(TC - TOC) \times 8.33$.

Data handling and statistical analysis

For statistical analyses, rare taxa (ostracods: taxa with less than 2% abundance in fewer than three samples; diatoms: taxa with less than 2% abundance in the samples) were excluded and relative abundances square root transformed. Samples containing fewer than 10 ostracod and 25 diatom valves were excluded as well. Hierarchical clustering (Bray–Curtis similarity index) to identify zone boundaries for ostracod and diatom

assemblages and principal component analyses (PCAs) (ter Braak 1983) to study trends in species composition were performed and displayed with PAST ver. 3.25 (Hammer *et al.* 2001). Transition zones (TZ) were defined based on hierarchical clustering as one or very few samples next to a barren section in the sequence. One single sample clearly separated by cluster analysis from neighbouring assemblage zones (AZ) was identified as event layer (E). Results were stratigraphically displayed using C2 ver. 1.7.7 (Juggins 2007).

Based on a modern training set applied to another Quaternary profile in central Germany by Pint *et al.* (2017), a salinity reconstruction was carried out based on samples from RP 13 II. The salinity transfer function ($R^2 = 0.74$, RMSEP = 0.9) relies on a merged data set of 26 modern samples from Central Germany (Pint *et al.* 2015) plus 47 from the southern Baltic Sea coast (Frenzel *et al.* 2010) and covers salinities from 0.1 to 6.1 (psu). A WAPLS model was applied. Only samples with at least 50 valves were analysed. Eight adjacent samples with fewer valves were placed into groups of two or three to reach the minimum number of shells if samples belonged to the same ostracod zone. Juvenile taxa and shell fragments with known higher taxon attribution were added to the corresponding species according to their adult proportions.

Five of the fossil taxa (*Neglecandona altoides*, *Candona weltneri*, *Fabaeformiscandona balatonica*, *Cyclocypris serena* and *Limnocytherina sanctipatricii*) are not covered by the modern training set. Because the two *Candona* species are prominent in many samples, the reliability of the reconstruction is probably reduced. We therefore added a mutual ostracod salinity range (MOSR) reconstruction sensu Pint *et al.* (2017) for cross-validation of results. Whereas the salinity transfer function gives mean values and error margins, the MOSR reconstructs minimum and maximum values based on salinity tolerances given in Meisch (2000) and Frenzel *et al.* (2010). An advantage of the MOSR is its better coverage of species but it is more dependent on the presence of single species.

To assess the ratio of turbulent and flowing water to calm water preferring ostracod species, the ostracod turbulence index (OTI) was calculated following Pint *et al.* (2015) (Eqn. 1). Rheoeuryplastic species were excluded from the calculation and *Cyclocypris serena* was also left out because this species is considered oligo-mesorheophilic (Meisch 2000).

$$\mathrm{OTI}\,(\%) = \frac{(\text{valves of mesorheophilic} + \text{polyrheophilic species}) \times 100}{(\text{valves of rheophobic} + \text{oligorheophilic} + \text{mesorheophilic} + \text{polyrheophilic species})} \quad (1)$$

In ostracod analyses, *Ilyocypris bradyi* morphotype (MT) 2 was separated from *I. bradyi* MT1 because valves of the former possess tubercles, a feature that can normally be observed on late juvenile but not on recent adult valves (Meisch 2000). Nonetheless, tuberculated adult specimens and transitional forms are documented (Mazzini *et al.* 2014) and individuals of *I. bradyi* with tubercles have also been reported from other Middle Pleistocene deposits in England (D. J. Horne, pers. comm. 2021). In addition to *Cyclocypris ovum*, small numbers of specimens of *Cyclocypris taubachensis* were observed. However, because transitional forms were present as well and Meisch (2000) placed *C. taubachensis* within the variability range of *C. ovum*, both taxa are discussed together as *C. ovum*.

Pollen data were re-evaluated using the TILIA software package (Grimm 1990). Local pollen assemblage zones (LPAZ) defined for sequences Schöningen 12 II and 13 II *s.l.* are based on conventional observation of the distribution and variation of the dominant taxa (Urban 1995, 2007; Urban & Bigga 2015; Kunz *et al.* 2017). The basic sum of calculations generally refers to the sum of arboreal (AP) and non-arboreal (NAP) pollen. Thermophile pollen in levels younger than 13 II-2c3 are interpreted as reworked palynomorphs. For validation of the LPAZ, a program for stratigraphically constrained cluster analysis (Grimm 1987) was applied to the pollen data of the Reference Profile (RP) 13 II in this paper. Furthermore, ecological groups were formed to better illustrate major changes of vegetation and environment (Fig. 6).

Results

Ostracod and charophyte developments

The ostracod abundance in RP 13 II (2003) is highly variable (0–1086 ostracod valves per gram dry weight (DW)) and preservation often poor (Fig. 2). Out of the 60 samples analysed, 31 samples were void of ostracods or contained fewer than 10 valves. Levels belonging to these barren sections are mainly 13 II-1 – lower part of sub-sublevel 13 II-2c4, upper part of 13 II-2c1–II-2b 2a (b), upper part of 13 II-4e3–II-4e1 and 13 II-5d2–II-5c2. A total of 20 ostracod species were found. Juvenile Candoninae and *Cyclocypris* spp. dominate the sequence. The most frequent species are *Cyclocypris ovum* (Jurine, 1820), *Pseudocandona compressa* (Koch, 1838), *Prionocypris zenkeri* (Chyzer & Toth, 1858), *Ilyocypris bradyi* Sars, 1890, *Cyclocypris laevis* (O.F. Müller, 1776) and *Limnocythere inopinata* (Baird, 1843) (Fig. 3). Both female and male specimens of *L. inopinata* were found. *Neglecandona altoides* Petkovski, 1961 shows a slightly variable shape with some specimens

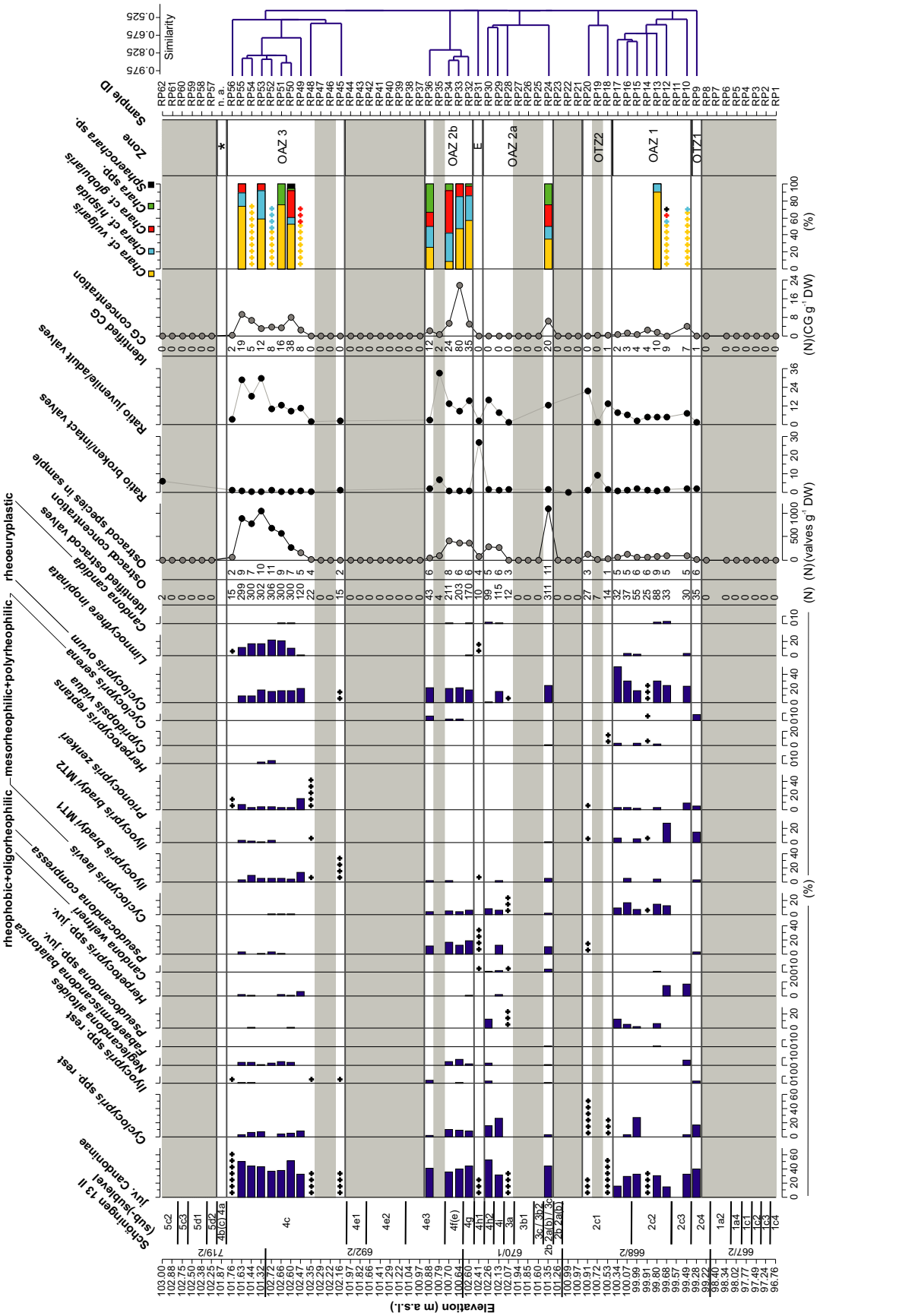
Elevation (m a.s.l.)
Schlotingen 13 II (sub-)sublevel
Juv. Candoninae
Cyclocypris spp. test
Ilyocypris spp. test
Negreccandona altoides
Fabaeformiscandona balatonica
Pseudocandona spp. juv.
Herpetocypris spp. juv.
Candona weltneri
Pseudocandona compressa
Cyclocypris laevis
Ilyocypris bradyi MT1
Ilyocypris bradyi MT2
Prionocypris zenkeri
Herpetocypris reptans
Cypridopsis vidua
Cyclocypris serena
Limnocythere inopinata
Candona candida
Identified ostracod valves
Ostracod concentration
Ostracod species in sample
rheoeuryplastic
mesorheophilic+polyrheophilic
rheophobic+oligorheophilic
Ratio broken/intact valves
Ratio juvenile/adult valves
Identified CG
CG concentration
Chara cf. vulgaris
Chara cf. hispida
Chara cf. globularis
Chara spp.
Sphaerochara sp.
Zone
Sample ID
Similarity
0.975
0.825
0.675
0.525
OAZ 3
OAZ 2b
OAZ 2a
OAZ 1
OTZ2
OTZ1
(%)
(N) (N)(valves g-1 DW)
(N)(CG g-1 DW)
(%)

Fig. 2. Ostracod (dark blue) and charophyte abundances of Reference Profile 13 II (2003) with results of the hierarchical cluster analysis. Ostracod taxa that occurred in more than two samples are included and differentiated as rheophobic + oligorheophilic, mesorheophilic + polyrheophilic and rheoeuryplastic ostracod species. DW = dry weight; CG = charophyte gyrogonites; OAZ = ostracod assemblage zone; OTZ = ostracod transition zone; E = event layer; n. a. = not analysed. In samples with less than 10% of the targeted individual counts (ostracods: 30 valves; charophytes: 10 gyrogonites), abundances are indicated semi-quantitatively with a plus. Grey dots in ostracod concentration curve indicate that fewer than 300 valves were identified, and grey areas show barren sections. Star indicates position of the 'Spear Horizon'.

possessing more elongated posterior ends. Gyrogonites of four charophyte taxa are present, with *Chara* cf. *vulgaris* Linnaeus, 1753 being dominant and *Chara* cf. *hispida* Linnaeus, 1753 and *Chara* cf. *globularis* Thuiller, 1799 co-occurring commonly. Additionally, very rare gyrogonites belonging to genus *Sphaerochara* were identified.

In sequence 12 II DB (2009), preservation is generally poor and aquatic microfossil abundance low (Fig. 4). Identifiable remains were only present in sub-sublevel 12 II-4c1 (14 samples), except for one ostracod valve in sub-sublevel 12 II-3c1 (DB18). Eleven ostracod species and gyrogonites of four charophyte taxa were found. The ostracod concentration varies between 0 and 298 valves per gram DW, while the concentration of charophyte gyrogonites ranges between 0 and 8 CG g^{-1} DW. Because of the poor preservation and missing identification characteristics, ostracod valves were often only identified to genus level. Juvenile Candoninae (60%) are dominant and *Cyclocypris* spp. and *Ilyocypris* spp. commonly co-occur. The most frequent ostracod species are *Herpetocypris reptans* Baird, 1835 (9.7%),

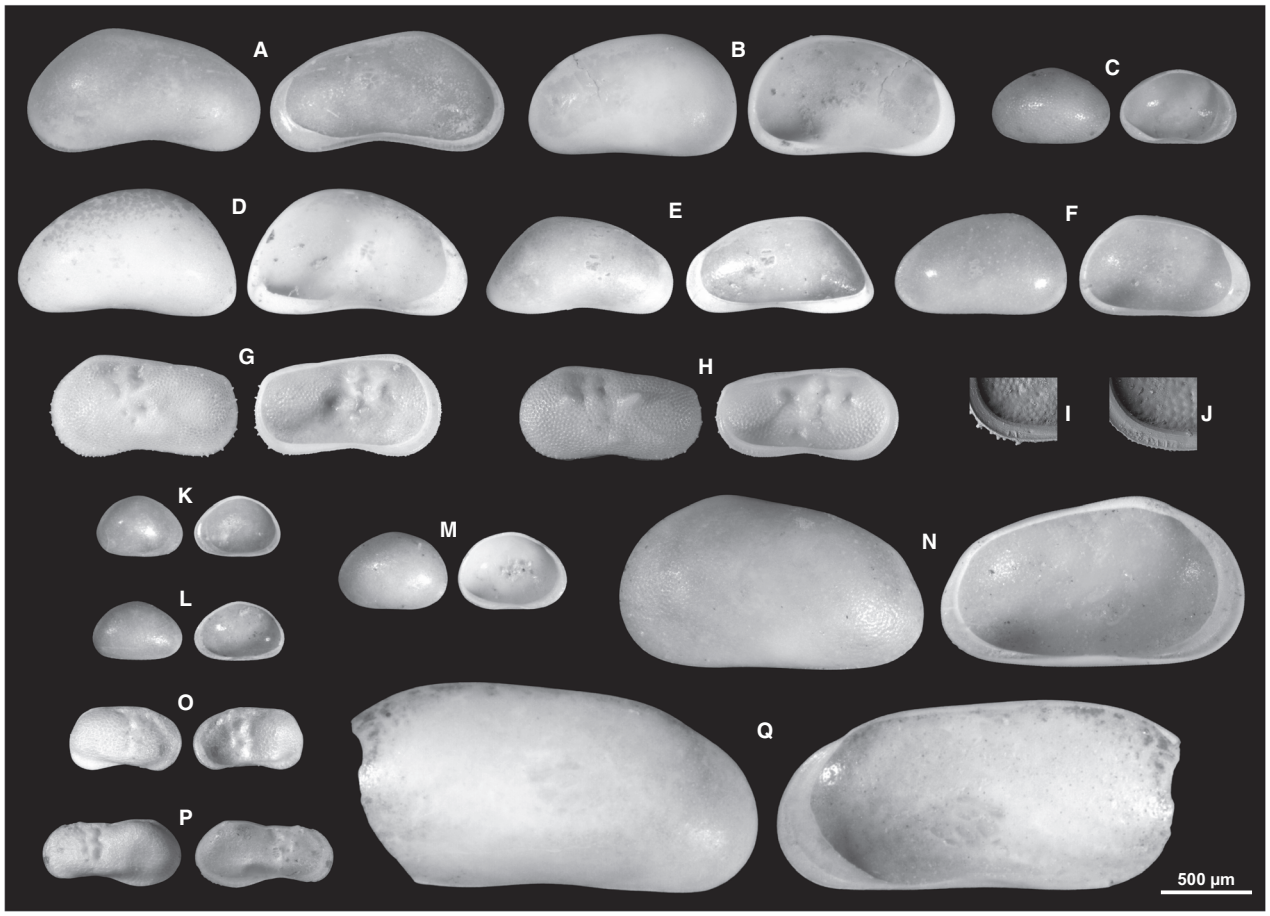

Fig. 3. Most abundant ostracod taxa in the Reinsdorf sequence. A. *Neglecandona altoides*, RV. B. *Candona weltneri*, LV. C. *Cypridopsis vidua*, LV. D. *Candona candida*, LV. E. *Fabaeformiscandona balatonica*, RV. F. *Pseudocandona compressa*, LV. G. *Ilyocypris bradyi* without spines MT1, LV. H. *Ilyocypris bradyi* with spines MT2, LV. I. *Ilyocypris bradyi* without spines MT1, LV, SEM detail image of PVMR (unscaled). J. *Ilyocypris bradyi* with spines MT2, LV, SEM detail image of PVMR (unscaled). K. *Cyclocypris laevis*, RV. L. *Cyclocypris ovum*, RV. M. *Cyclocypris serena*, LV. N. *Prionocypris zenkeri*, LV. O. *Limnocythere inopinata*, RV, female. P. *Limnocythere inopinata*, LV, male. Q. *Herpetocypris reptans*, RV. RV = right valve; LV = left valve; SEM = scanning electron microscope; PVMR = postero-ventral marginal ripplets.

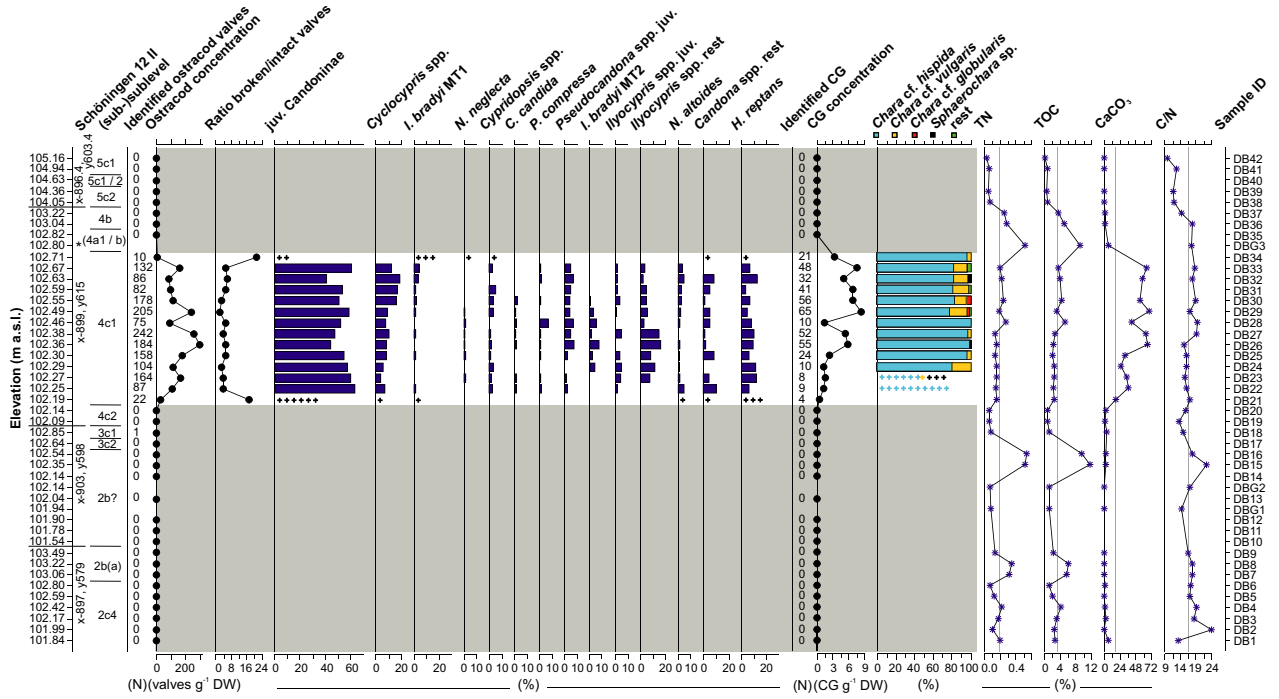

Fig. 4. Ostracod, charophyte and geochemistry record of 12 II DB (2009). Grey lines in geochemical data columns show mean value of the sequence. Grey areas show barren sections. In samples with less than 10% of the targeted individual counts (ostracods: 30 valves; charophytes: 10 gyrogonites), abundances are indicated semi-quantitatively with a plus. DW = dry weight. Star indicates level corresponding to the 'Spear Horizon'.

I. bradyi MT1 (3.6%) and *Neglecandona altoides* (2.1%). The ratio of broken to intact valves is highest at the beginning and end of sub-sublevel II-4c1. *Chara* cf. *hispida* clearly dominates the charophyte assemblage (86.9%).

Based on hierarchical clustering, a differentiation in RP 13 II into three ostracod assemblage zones (OAZ1–3), two subzones (OAZ2a/2b), two ostracod transition zones (OTZ1/2) and one event layer (E) was made.

The lowermost ostracod sample (OTZ1, sub-sublevel 13 II-2c4) is comprised of higher abundances of juv. Candoninae and *Cyclocypris* spp., *Ilyocypris bradyi* MT2 and *Cyclocypris serena* (Koch, 1838). The calculated ostracod turbulence index (OTI) amounts to 50%.

OAZ1 (sub-sublevels 13 II-2c3 – beginning of 13 II-2c1) is characterized by low ostracod concentrations (80 valves g^{-1} DW on average). Characteristic species of this zone are *I. bradyi* MT2 (up to 27.3%), *Cypridopsis vidua* (O.F. Müller, 1776) (up to 14.3%), *Fabaeformiscandona protzi* (Hartwig, 1898) (up to 8.0%) and *Darwinula stevensoni* (Brady & Robertson, 1870) (up to 1.8%), which only occur in low abundances in the other zones if at all. The ratio of broken to intact (B/I) valves ranges between 0.6 and 1.9, while the juvenile/adult (J/A) ratio varies between 2.5 and 7.5. Values of the OTI are high (75–100%). Gyrogonites of charophytes (CG) are only found in low concentrations in the lower part of OAZ1 and dominated by *Chara* cf. *vulgaris* (maximum 90%).

The succeeding OTZ2 (central section of sub-sublevel 13 II-2c1) is comprised of three samples, of which one is almost barren. Juvenile Candoninae (25.9–57.1%) and unidentifiable *Cyclocypris* spp. (28.6–55.6%) dominate OTZ2. *Pseudocandona compressa* occurs with higher abundances (11.1%).

OAZ2a (sublevels 13 II-2b 2a(b)/3c–II-4h2) is marked in the beginning (sublevels 13 II-2b 2a(b)/3c, 101.35 m a.s.l., square 670/1) by the highest ostracod concentration (1086 valves per gram DW). *Pseudocandona compressa* remains common (10.6%). The following three samples (sublevels 13 II-3c/3b2–II-3b1) document a phase void of ostracods. The upper part of OAZ2a (sublevels 13 II-3a–II-4h2) is characterized by increased abundances of *Pseudocandona* spp. (average 17.1%) and *Candona weltneri* Hartwig, 1899 (4.0%). The ostracod concentration (5–277 valves per gram DW) and the J/A ratio (1.4–15.9) increase therein towards the top. OTI values are low and range between 0 and 30%.

Sub-sublevel 13 II-4h1 (E, 102.41 m a.s.l., square 670/1), separating OAZ2a and 2b, shows a significant increase in the B/I ratio (26.7) and a low J/A ratio (2.6). *Pseudocandona compressa* is the most dominant species (40%), while juvenile *Candona* spp., *C. weltneri*, *I. bradyi* MT1 and *L. inopinata* frequently co-occur.

With the onset of OAZ2b (sublevels 13 II-4g – lower part of 13 II-4e3) ostracod concentrations along with the J/A ratio increase again, while the B/I ratio decreases. *Pseudocandona compressa* still occurs frequently (aver-

age 16.3%) and the relative abundance of *Neglecandona altoides* increases (up to 7.9%). Lowest values were calculated for the OTI (0–17%). Gyrogonites of charophytes reach a maximum concentration of 21.6 CG per gram DW.

OAZ3 (sublevel 13 II-4c) is marked by a distinct change in species composition. The ostracod concentration is comparatively high with a maximum of 1046 valves g^{-1} DW and up to 11 different species occur. Numbers of juvenile valves (J/A ratio: 29.7) increase and the OTI shows again higher values of between 79 and 100%. Average relative abundances of *L. inopinata* (10.8%), *P. zenkeri* (10.1%) and *I. bradyi* MT1 (9.2%) increase, while *P. compressa* is rare. *Chara* cf. *vulgaris* is again the most dominant taxa (on average 70.3%).

Salinity reconstruction

Only 15 samples of RP 13 II contained enough valves to apply the salinity transfer function (TF). Seven other samples were merged to three samples thus leaving 18 levels for salinity reconstruction in total. The reconstructed salinity varies between 0.6 and 2.8 (psu) with an increase in OAZ2a and a maximum in OAZ2b within the β-oligohaline range (0.5–3 (psu)) of the classification of brackish waters (Fig. 8). Salinities reconstructed by the ostracod-based TF correspond to ranges indicated by MOSR. The error ranges of the reconstructed TF values of all samples are overlapping making absolute values less reliable. The clear trends of increased values in OAZ2 and their reflection by MOSR, however, confirm the results.

Diatom assemblages

The diatom concentration in RP 13 II ranges from 0–119×10^6 valves per gram DW and 33 out of the 59 analysed samples are void of diatoms or almost barren (sub-sublevels 13 II-1a2 – lowermost part of 13 II-2c1, 13 II-4e2 – central part of 13 II-4c, 13 II-5d2–II-5c2) (Fig. 5). In total, 194 diatom taxa were identified. Despite the high number of benthic species, only tycho-

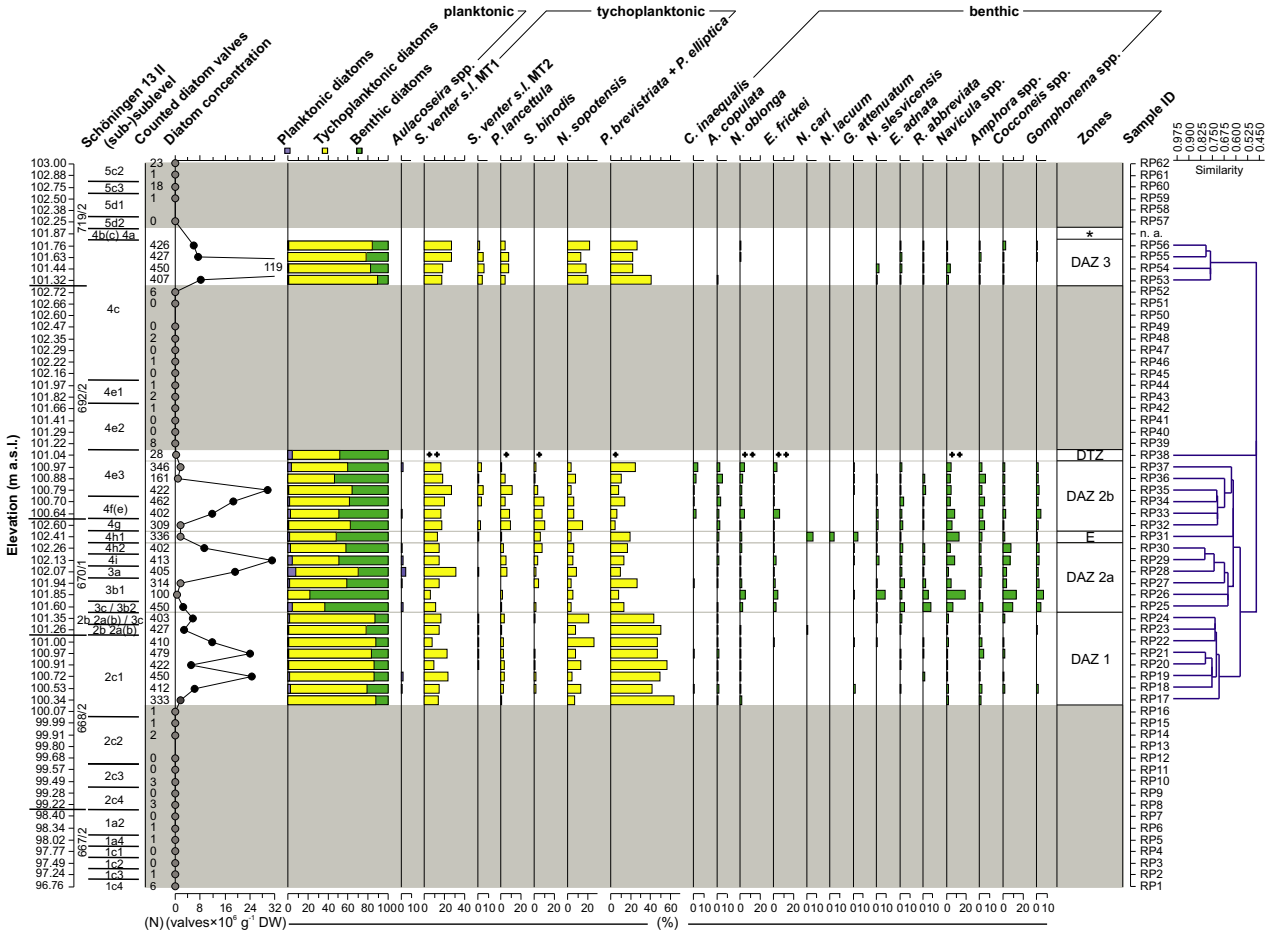

Fig. 5. Diatom record of Reference Profile 13 II (2003) with relative abundances of most abundant taxa and results of hierarchical cluster analysis (zones). In samples with less than 10% of the targeted individual counts (40 valves), abundances are indicated semi-quantitatively with a plus. DW = dry weight; DAZ = diatom assemblage zone; E = event; DTZ = diatom transition zone; n. a. = not analysed. Grey areas show barren sections. Grey dots in diatom concentration indicate samples with fewer than 400 valves counted. Star indicates position of the 'Spear Horizon'.

planktonic taxa, e.g. *Pseudostaurosira brevistriata* (Grunow) D.M. Williams & Round, 1988, *Pseudostaurosira elliptica* (Schumann) Edlund, Morales & Spaulding, 2006 and *Staurosira venter* (Ehrenberg) Cleve & J.D. Möller 1879 *s.l.*, are dominant. Planktonic taxa occur only occasionally. Diatom samples in sequence 12 II DB (2009) did not yield enough valves for a reliable reconstruction.

Hierarchical clustering resulted in the differentiation of three main diatom assemblage zones (DAZ1–3) in RP 13 II, two subzones (DAZ2a/2b), one diatom transition zone (DTZ) and one event layer (E).

In DAZ1 (sub-sublevels 13 II-2c1–II-2b 2a(b)/3c), the relative abundance of tychoplanktonic diatoms remains constantly high (average 83.3%). Dominating taxa are *P. brevistriata* and *P. elliptica*, which constitute together half of the assemblage. *S. venter s.l.* MT1 (15.3%) and *Nanofrustulum sopotensis* (Witkowski & Lange-Bertalot) E. Morales, C.E. Wetzel & Ector, 2019 (12.9%) are also frequently present. The diatom concentration shows large variations (1.8–24.5 valves×10^6 per gram DW).

The onset of DAZ2a (sublevels 13 II-3c/3b2–II-4h2) is marked by a sudden increase in benthic taxa, especially of *Navicula* spp. (up to 19%), *Cocconeis* spp. (up to 13%) and *Gomphonema* spp. (up to 7%) and highest abundances of planktonic taxa (maximum 7.7%, mostly *Aulacoseira* spp.). *Rhoicosphenia abbreviata* (C. Agardh) Lange-Bertalot, 1980, *Navicula slesvicensis* Grunow, 1880 and *Epithemia adnata* (Kützing) Brébisson, 1838 are the most frequent benthic species. Moreover, *Punctastriata lancettula* (Schumann) P.B. Hamilton & Siver, 2008 and *Staurosira binodis* (Ehrenberg) Lange-Bertalot, 2011 increase in abundances. The diatom concentration is low at the beginning of OAZ2a (sublevels 13 II-3c/3b2–II-3b1, 0.5–2.5 valves×10^6 per gram DW) but increases towards the top (up to 31.1 valves×10^6 per gram DW).

A significant drop in diatom concentration (1.78 valves×10^6 per gram DW) can be observed in sub-sublevel 13 II-4h1 (102.41 m a.s.l., square 670/1). Moreover, this distinct horizon (E) is characterized by the one-time occurrence of *Navicula lacuum* Lange-Bertalot, Hofmann, Werum & Van de Vijver, 2009 as well as increased abundances of *Navicula cari* Ehrenberg, 1836 (6.3%) and *Gyrosigma attenuatum* (Kützing) Rabenhorst, 1853 (4.8%), species which rarely occur in the other samples.

In the succeeding DAZ2b (sublevels 13 II-4g – lower and central part of 13 II-4e3), benthic taxa are still present (average 42.5%). However, several benthic taxa frequent in DAZ2a decrease in abundances, while *Amphora* spp. (average 4.2%) and *Cymbopleura inaequalis* (Ehrenberg) Krammer, 2003 (average 1.9%) occur more often. Diatom concentrations initially increase in DAZ2b up to the central part (maximum 29.7 valves×10^6 per gram DW) and drop again suddenly afterwards.

The DTZ (uppermost part of sublevel 13 II-4e, 101.04 m a.s.l., square 692/2) is almost barren (0.15 valves×10^6 per gram DW) and followed by a long section of poor diatom preservation. Several common taxa disappear, while *Navicula oblonga* (Kützing) Kützing, 1844 (10.7%) and *Epithemia frickei* Krammer, 1987 (10.7%) become more abundant.

In DAZ3 (upper part of sublevel 13 II-4c) highest diatom concentrations are documented (119 valves×10^6 per gram DW), and benthic taxa are replaced by the tychoplanktonic taxa dominating DAZ1 (average 82.5%).

Statistical validation of local pollen assemblage zones

The results of the pollen data cluster analysis are plotted together with selected pollen groups which reflect the status and development of vegetation in more detail. Cluster analysis and distribution and variation of the dominant taxa identify four main clusters and eight local pollen assemblage zones (LPAZ) in Reference Profile 13 II (Fig. 6).

The first cluster separates LPAZ R3a, R3b (thermal maximum) and R4/5 from the upper part of the profile. This lowermost cluster ends with the last occurrence of thermophile woody taxa. LPAZ RP1, beginning with sub-sublevel 13 II-2c3 and ending with sub-sublevel 13 II-2c1, is defined by the second cluster. Indifferent woody taxa decrease (~25%), while terrestrial herbs as well as Poaceae increase.

A third cluster separates LPAZ RP2a to LPAZ RP3 from the upper part of the profile. This separation is based on a higher proportion of tree and shrub pollen of the indifferent woody taxa group. The fourth cluster groups RP4a with RP4b, and RP5 with RP6. The first group is characterized by a drop and subsequent rise of tree and shrub pollen of indifferent woody taxa and a higher proportion of terrestrial herbs (RP4a and RP4b). The second group of this cluster is separated by a further rise of terrestrial herbs and a strong decrease of indifferent woody taxa such as *Pinus* and *Betula* (RP5 and RP6).

Ordination of aquatic microfossil data

The variance explained by the first and second component of the PCA of the ostracod data set in RP 13 II is 22.9 and 18.2%, respectively (Figs 7, 8). Comparison with the broken-stick model shows that the first five components can be regarded as significant and bear relevant information. The PCA biplot shows three clusters, which mainly correspond to the OAZ determined by hierarchical clustering (Fig. 7A). *Cyclocypris* species are strongly associated with component 1, which also separates OAZ1 and 3. *Pseudocandona compressa* is connected to positive values of component 2 (OAZ2a/2b), whereas *Prionocypris zenkeri*, *Limnocythere inopinata* and *Ilyocypris bradyi* are oriented towards negative values (OAZ1/3).

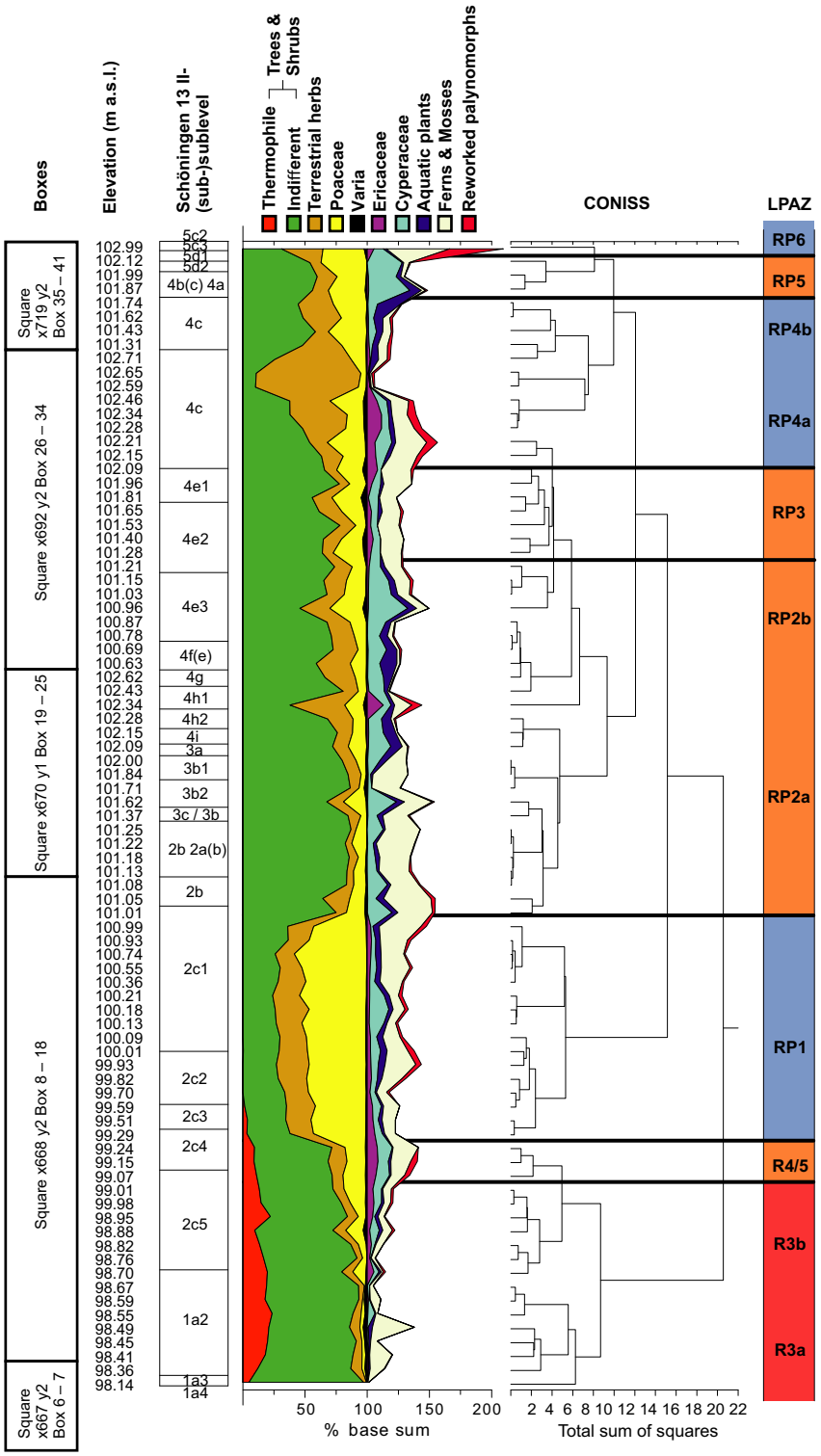

Fig. 6. Group-clustered pollen record and local pollen assemblage zones (LPAZ) of the Reference Profile (RP) 13 II (2003) based on palynological analysis (Urban & Bigga 2015). Base sum of the pollen groups is defined by trees & shrubs, terrestrial herbs, Poaceae and Varia (= 100%). Thermophile tree, shrub and other wooden taxa mainly include *Corylus*, *Quercus*, *Ulmus*, *Tilia*, *Carpinus*, *Abies*, *Hedera* and *Ilex*. Thermophile pollen in levels younger than 13 II-2c3 are interpreted as reworked palynomorphs. The green curve represents mainly *Betula*, *Alnus*, *Salix*, *Populus*, *Pinus*, *Picea*, *Juniperus* and *Larix*. LPAZ: red = warm interglacial, thermophile, deciduous dominated forests; orange = cool-temperate, boreal forest-steppe; blue = cool, steppe and open forest-steppe.

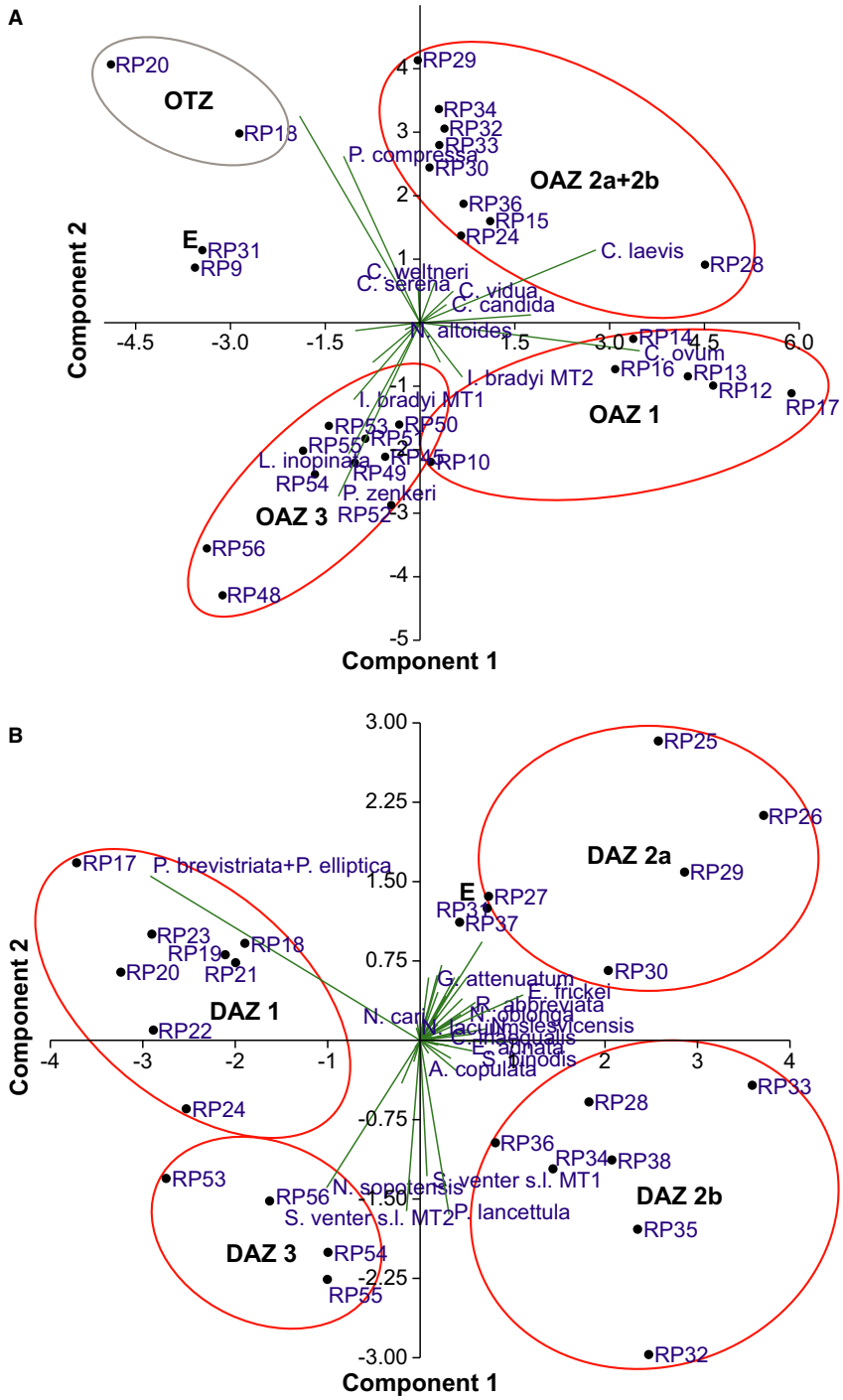

Fig. 7. Principal components analysis (PCA) biplot of ostracod (A) and diatom (B) taxa (arrows) and samples (circles) of components 1 and 2 (explained variance ostracods: component 1: 22.9%, component 2: 18.2%; explained variance diatoms: component 1: 32.7%, component 2: 13.1%) of Reference Profile 13 II (2003). Only species presented in Figs 2 and 3 are labelled. Red circles indicate ostracod (OAZ) and diatom (DAZ) assemblage zones determined by hierarchical clustering. Grey circle marks the ostracod transition zone (OTZ). E = event layer.

In the diatom data set, the first four components determined by PCA explain a significant portion of the variance (component 1: 32.7%, component 2: 13.1%). Four clusters, which mainly coincide with the DAZ defined by hierarchical clustering, are displayed in the PCA biplot (Fig. 7B). Component 1 mainly separates tychoplanktonic (more negative values, DAZ1/3) from benthic taxa (more positive values, DAZ2a/2b). Positive values of component 2 are strongly associated with *Pseudostaurosira brevistriata* + *P. elliptica* and negative

values with *Staurosira venter s.l.*, *Punctastriata lancettula* and *Nanofrustulum sopotensis*.

Changes in the TN, TOC, $CaCO_3$ and C/N records

The Reinsdorf deposits are marked by considerable, often opposing variations in $CaCO_3$ and TOC contents (Figs 4, 8). TN and TOC show similar trends in both sequences and C/N ratios generally decline towards the top.

Highest TN and TOC values in RP 13 II occur from sublevel 13 II-2b 2a(b)/3c to the beginning of sub-sublevel 13 II-4e2, with a maximum of 0.9% (TN) and 16.2% (TOC) in sub-sublevel 13 II-4h1 (Fig. 8). Additionally, values are generally higher between sublevels II-3c/3b2 and 13 II-4h1.

Increased $CaCO_3$ contents are recorded in sublevel 13 II-2b 2a(b)/3c (75.7%), sublevels 13 II-4i up to the beginning of 13 II-4e3 (~50%) and the upper part of sublevel 13 II-4c (~56.8%). Sub-sublevels 13 II-2c3 to II-2c1 are characterized by slightly increased values (9.1–19.6%), whereas especially sub-sublevels 13 II-4e3 (upper part) to II-4e1 and level II-5 show very low $CaCO_3$ contents (<3.2%).

Slight increases in C/N ratios are detected at the transition of sub-sublevels 13 II-2c2 to II-2c1 (19–20) and between sublevel 13 II-3c/3b2a and the beginning of sub-sublevel 13 II-4e3 (17–19). The latter roughly corresponds to increased TN and TOC contents. Lowest values are found in sub-sublevel 13 II-5c2 (6–9).

Sequence 12 II DB (2009) is characterized by high variation in TOC content, exhibiting values in the range of 0.3–11.6% (Fig. 4). Highest values were recorded in level 12 II-2b(a), in the upper part of level 12 II-2b? and in level 12 II-4a1/b. Especially the uppermost part of the sequence exhibits low TOC values (0.3–0.9%). Overall, the TOC development roughly correlates with TN (0.03–0.5%).

The $CaCO_3$ content is generally very low (<6.5%), except for sub-sublevel 12 II-4c1 with values varying between 17.2 and 67.4%.

C/N ratios vary between 10 and 24 and show temporary increases in the middle of sub-sublevel 12 II-2c4 (24), at the top of sublevel 12 II-2b? (up to 22) and in the upper part of sub-sublevel 12 II-4c1 to II-4b (17–19). High C/N ratios in sublevel 12 II-2b? correspond to highest TOC and TN contents.

Discussion

Preservation of aquatic microfossils in the Reinsdorf deposits

Aquatic microfauna in the Schöningen record shows markedly variable concentrations with temporarily either ostracods or diatoms present (Fig. 8), attesting to changing preservation conditions. Because diatoms and ostracods are present in almost all types of aquatic habitats, their absence in more than half of the samples suggests that post-mortem dissolution of ostracod and diatom valves and repeated silting up of the site likely took place. Although sample processing could have also caused damage, we considered this aspect as being minor as procedures were uniform for all samples of the sequence. Low concentrations of calcareous remains often coincide with increased organic matter contents, causing an acidic pH (Urban & Bigga 2015; Kunz *et al.* 2017) and probably postdeposition dissolution of ostracods in the Reinsdorf deposits related to silting up. The delayed appearance of diatoms compared to ostracods in parts of the record (e.g. level 13 II-4c) was possibly caused by a high pH of lake water related to increased fluvial input of carbonate-rich matter from the catchment and resulting dissolution of silicious diatom valves.

High numbers of broken ostracod and diatom valves suggest physical wear of the fossil assemblages in a high-energy environment and drying-out of sediments. Especially large pennate diatom species show increased damage, while small-celled taxa are generally better preserved. Mechanical breakage of diatoms is often attributed to shallow conditions with turbulent mixing and drying (Flower 1993; Ryves *et al.* 2006). Juvenile ostracod valves are generally more easily transported under high-energy conditions (Lord *et al.* 2012) and increased abundances of juveniles (J/A ratio up to 30, sublevel 13 II-4c) could therefore indicate deposition of allochthonous valves through incoming streams close to the study sites.

Physico-chemical palaeolake properties

Littoral ostracod species (e.g. *Pseudocandona compressa*), tychoplanktonic diatoms and charophyte gyrogonites commonly occur in the Reinsdorf sequences, mostly indicating shallow waters. The presence of charophytes in general suggests a water depth of at least 50 cm. *Chara vulgaris* and *Chara globularis* are indicative of shallow waters and develop usually between 0.5 and 2 m but possibly down to 4–6 (10) m water depth (Corillion 1957; Soulié-Märsche *et al.* 2010). The cosmopolitan *C. vulgaris* prefers the littoral zones of great lakes (Korsch 2016), whereas *Chara hispida* mainly occurs in deeper parts of lakes mostly below 2 m water depth (Pichler 1997; Langangen 2007; Soulié-Märsche *et al.* 2008). These depth ranges correspond to the results of other water plant remains found in level 13 II-4 (Bigga 2018). The occurrence of the calcified fructifications additionally confirms a continuous submersion of at least 3 months at the site (Soulié-Märsche 1991; Soulié-Märsche & García 2015). In general, the formation of gyrogonites is proposed to be more frequent in shallower water and might be forced by unstable environments (Soulié-Märsche & García 2015). A predominantly shallow water

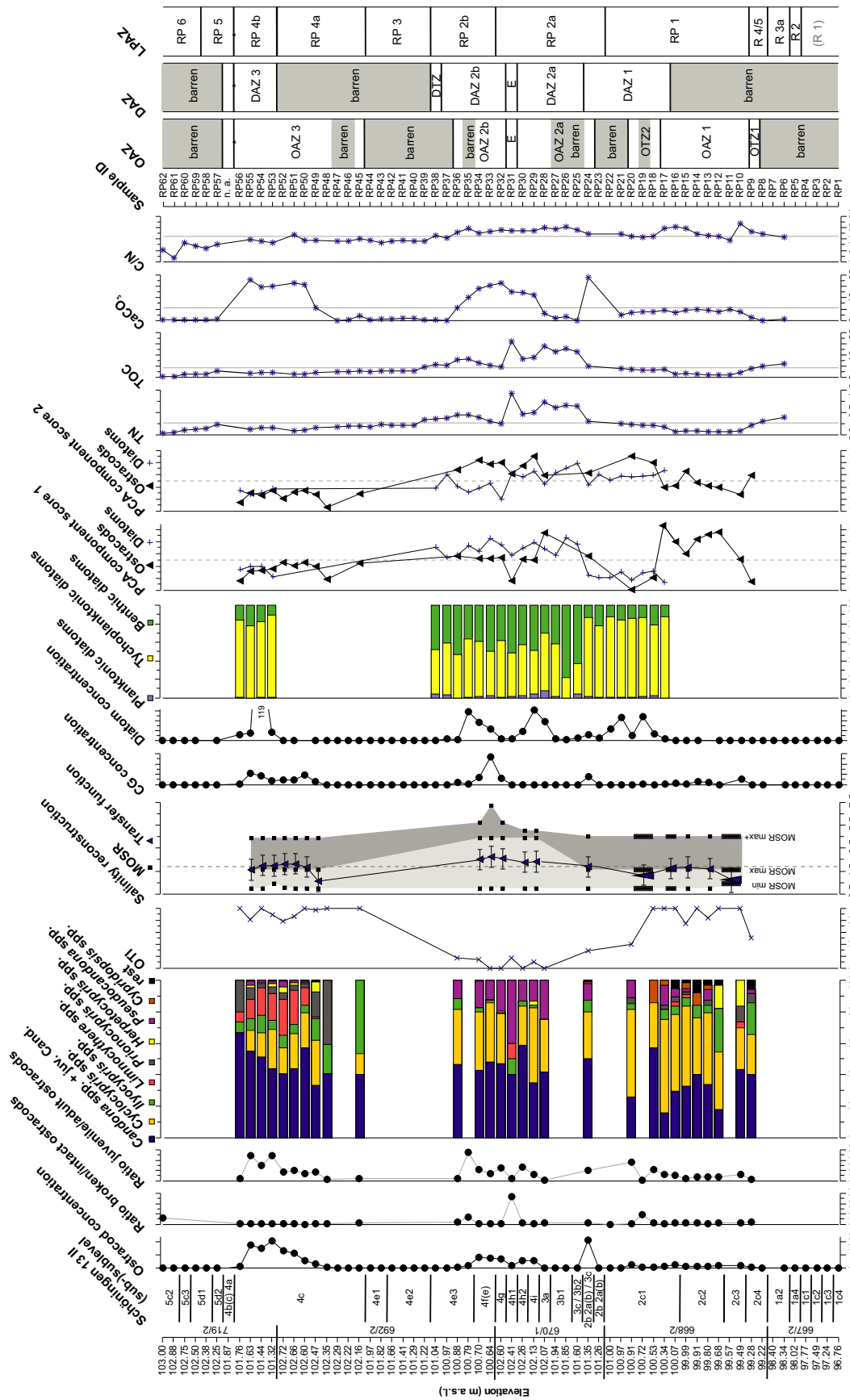
Schönlingen 13 II
(Sub-)Subliveal
Ostracod concentration
Ratio broken/intact ostracods
Ratio juvenile/adult ostracods
Candona spp. + juv. Cand.
Cyclocypris spp.
Ilyocypris spp.
Limnocythere spp.
Prionocythere spp.
Herpetocypris spp.
Pseudocandona spp.
Cyprinotus spp.
Candona spp.
Test OTI
Salinity reconstruction
MOSR
Transfer function
CG concentration
Diatom concentration
Planktonic diatoms
Tychoplanktonic diatoms
Benthic diatoms
PCA component score 1
Ostracods
Diatoms
PCA component score 2
Ostracods
Diatoms
TN
TOC
CaCO3
C/N
Sample ID
OAZ
DAZ
LPAZ
Elevation (m a.s.l.)
(valves g-1 DW)
(%)
(psu)
(CG g-1 DW)(valves×10^6 g-1 DW)(%)
MOSR max+
MOSR max
MOSR min
119
barren
OAZ 3
OAZ 2b
OAZ 2a
OAZ 1
OTZ2
OTZ1
DAZ 3
DAZ 2b
DAZ 2a
DAZ 1
DTZ
E
RP 6
RP 5
RP 4b
RP 4a
RP 3
RP 2b
RP 2a
RP 1
R 4/5
R 3a
R2
(R 1)
5c2
5c3
5d1
5d2
4b(c) 4a
4c
4e1
4e2
4e3
4f(e)
4g
4h1
4h2
4i
3a
3b1
3c / 3b2
2b 2a(b) / 3c
2b 2a(b)
2c1
2c2
2c3
2c4
1a2
1a4
1c1
1c2
1c3
1c4
719/2
692/2
670/1
668/2
667/2

Fig. 8. Synthesis of biological and geochemical proxies of Reference Profile 13 II (2003). Salinity reconstruction based on an ostracod-based transfer function, given with error ranges and mutual ostracod salinity range (MOSR) based on salinity ranges of the occurring ostracod taxa. The MOSR max+ limit relies on unusually high limits from the literature. Samples with counts of fewer than 50 valves are omitted. Elongated symbols show merged samples. Grey lines in salinity transfer function and geochemical data columns show mean value of the sequence. Dashed lines in PCA component scores 1 and 2 results show zero-point value. DW = dry weight; OTI = ostracod turbulence index; CG = charophyte gyrogonites; OAZ/DAZ = ostracod/diatom assemblage zone; E = event layer; OTZ/DTZ = ostracod/diatom transition zone; LPAZ = local pollen assemblage zone; n. a. = not analysed. R1 is available from corresponding profiles. Star indicates the position of the 'Spear Horizon'.

body is also supported by the mollusc fauna of Schöningen 13 II (Mania 2007b).

Furthermore, *Prionocypris zenkeri*, which avoids standing and deep waters (Meisch 2000), and several other mesorheophilic ostracod species suggest periods of slow flowing streams. The diatom *Epithemia adnata* is found in running waters, too, and *Navicula slesvicensis* prefers alkaline flowing freshwater habitats (Lange-Bertalot *et al.* 2017). Temporary influence of running waters was also deduced from the occurrence of, for example, the fish species burbot (*Lota lota*) (Böhme 2015).

Rich aquatic vegetation with abundant charophytes is documented in many parts of RP 13 II by the presence of gyrogonites and the ostracod species *Cypridopsis vidua* and *P. zenkeri* (Meisch 2000), together with epiphytic diatom taxa such as *Cocconeis* spp. and *E. adnata* (Lange-Bertalot *et al.* 2017). Results are supported by abundant remains of littoral macrophytes (e.g. *Nuphar lutea*, *Phragmites*, *Typha*) recorded by pollen (Urban 1995, 2007) and plant macro-remains (Jechorek 2000; Bigga 2018).

Many common diatom species in RP 13 II are classified as meso-eutraphentic to eutraphentic (van Dam *et al.* 1994) and suggest a rich supply of nutrients. However, the charophyte *C. hispida* mainly occurs in the oligo- to mesotrophic range, while *C. vulgaris* and *C. globularis* also tolerate higher nutrient levels (van de Weyer & Doege 2016). Macrophyte analyses point to meso- to eutrophic conditions (Bigga 2018) as well and fish remains indicated temporary eutrophication of the palaeolake (Böhme 2015).

Charophyte taxa suggest rather freshwater conditions, although *C. vulgaris* and *C. globularis* are known as halotolerant and may occur in the oligohaline range of salinity (generally <5 g L^{-1} of chlorite; García 1994; García & Chivas 2006). Moreover, *C. hispida* was only rarely reported from brackish water (Langangen 2007; Schubert *et al.* 2016). The documented ostracod species commonly occur in freshwater environments as well; however, several taxa such as *P. compressa* and *Limnocythere inopinata* prefer oligohaline to mesohaline waters (Meisch 2000) and thereby hint at increased salinities. Additionally, the ostracod-based salinity transfer function yields values within the β-oligohaline range. A slight influence of brackish waters is also visible by the presence of fresh-brackish (e.g. *Epithemia frickei*, *Navicula cari*, *Saurosira venter*) and brackish-fresh (e.g. *N. slesvicensis*) diatom species (van Dam *et al.* 1994). Furthermore, salt influencing the palaeolake was derived from increased soluble salt contents measured in the Reinsdorf deposits (Urban & Bigga 2015), and the occurrence of salt-tolerant plants (Jechorek 2000; Bigga 2018). The Reinsdorf sequence was deposited within a rim syncline, developed along the edge of the Helmstedt-Staßfurt salt wall (Brandes *et al.* 2012). Elevated salinities in the Schöningen deposits are thereby possibly connected to groundwater discharge influenced by this nearby salt wall into the lake.

Diatoms from RP 13 II are represented by several alkaliphilous and alkalibiont taxa (e.g. *Pseudostaurosira brevistriata*, *S. venter*, *Gyrosigma attenuatum*, *E. adnata*) reflecting high lake water pH. The ostracod *L. inopinata* was also found in alkaline pools (Löffler 1959) and Löffler (1990) discusses elevated alkalinity as a reason for male occurrences. Males of *L. inopinata*, commonly present in sublevel 13 II-4c of the Reinsdorf sequence, are extremely rare in central Europe today (Meisch 2000), but they were, for example, abundantly found in Germany in Eemian deposits and also occur in MIS 9 deposits (Horne & Martens 1999; Fuhrmann 2012; Bridgland *et al.* 2013).

Increased calcium content of lake waters is supported by the ostracod taxa. Although many species are titanoeuryplastic, several meso-polytitanophilic taxa point to at least 18 mg Ca L^{-1} (e.g. *Ilyocypris bradyi*, *P. compressa*). *Prionocypris zenkeri* and *Cyclocypris serena* even suggest a calcium content of more than 72 mg L^{-1} (Meisch 2000). However, considering its preference for streams, *P. zenkeri* might be allochthonous and possibly documents the calcium content of inflows from the Elm and not in the palaeolake.

Comparison of lake-shore characteristics between sites 12 II DB and 13 II

Integration of sites 12 II DB and 13 II allows a better differentiation between local signals and general environmental developments.

Overall, not all levels documented in RP 13 II can be found in sequence 12 II DB (2009) and thickness of the individual levels varies between the sites (Tables S1, S2). Missing, probably eroded, levels and the poorer preservation of aquatic microfossils in 12 II DB compared to RP 13 II generally indicate more disturbances at site 12 II

DB. Sand horizons recorded at site 12 (Profile Schöningen 12 B) point to temporarily increased fluvial activity (Urban & Sierralta 2012).

The ostracod species composition is similar in both sequences, although abundances of individual taxa vary. Considering their common location close to the lake shore at an approximate distance of 1–2 km (Fig. 1B), this is not surprising. Mesorheophilic species (e.g. *Ilyocypris bradyi*, *Herpetocypris reptans*) indicate flowing waters at both sites, thereby complementing sedimentological results (e.g. Julien *et al.* 2015). Slightly higher abundances of *Pseudocandona compressa* and

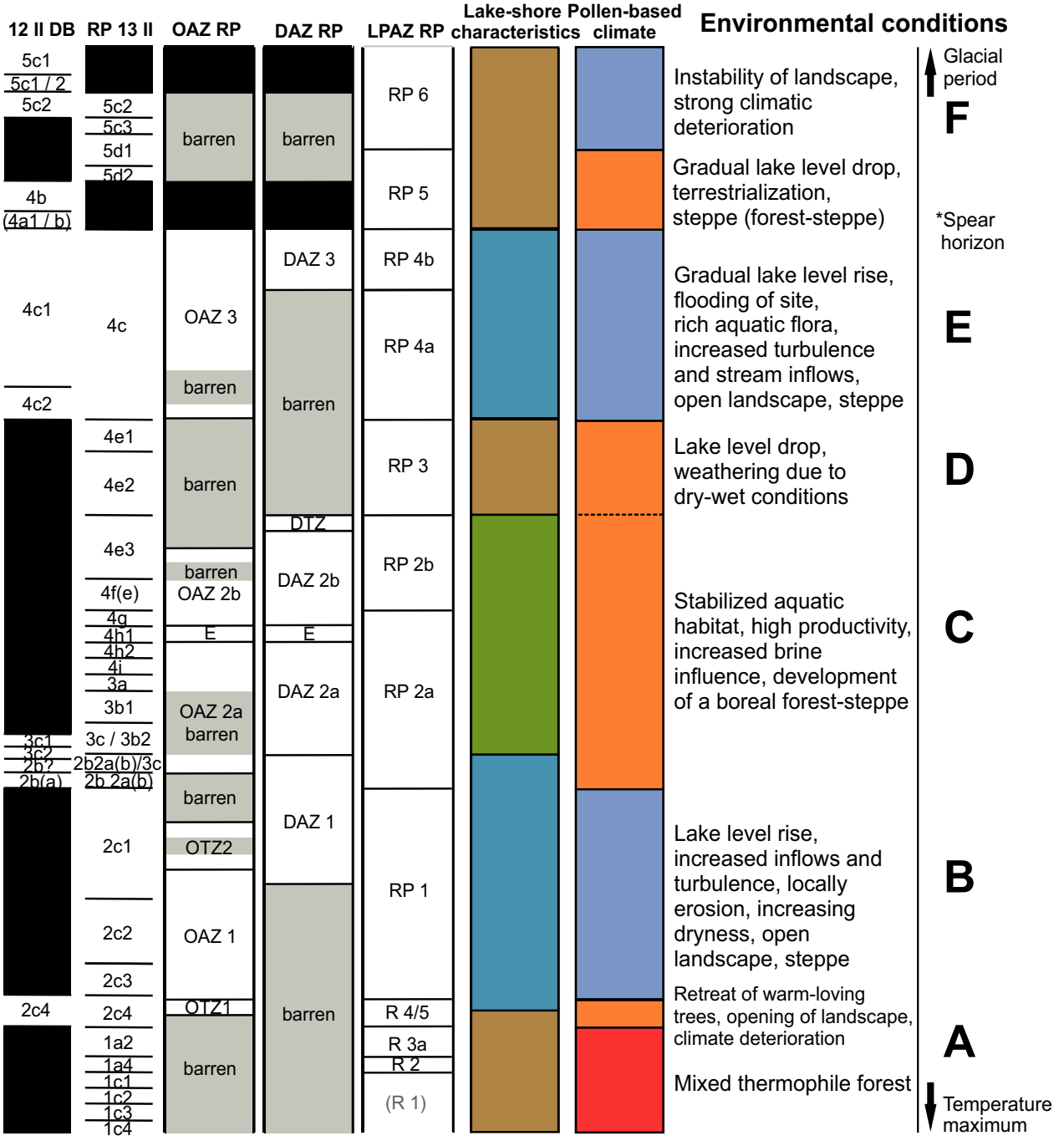

Fig. 9. Environmental development at the palaeolake shore in Schöningen during the Reinsdorf sequence showing (sub-)sublevel of sequence 12 II DB (2009) and Reference Profile 13 II (2003), inferred aquatic microfossil development zones (OAZ, DAZ) combined with local pollen zones (LPAZ), major lake-shore developments (brown = dry or temporarily flooded; blue = higher water levels and increased erosion caused by pronounced stream inflows; green = more stable, shallow aquatic conditions with increased productivity and salinity) and vegetation-inferred climatic conditions (red = warm interglacial; orange = cool-temperate; blue = cool). Letters A–F correspond to diagrams in Fig. 10.

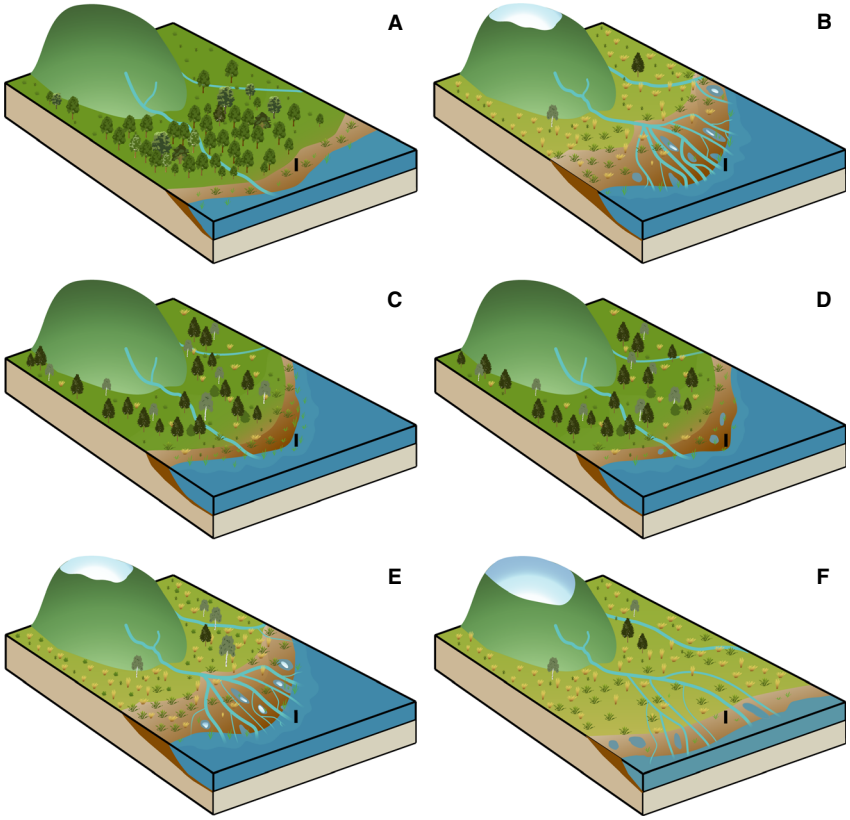

Fig. 10. Simplified, unscaled model of environmental changes throughout the Reinsdorf sequence close to Reference Profile 13 II (black bar). A. Thermal optimum, dry or temporarily flooded, thermophile, deciduous dominated forests. B. Increased water levels with pronounced stream inflows, cool conditions, steppe. C. Less turbulence and more stable, shallow aquatic conditions with increased productivity and salinity, cool-temperate, boreal forest-steppe. D. Dry or temporarily flooded, cool-temperate, boreal forest-steppe. E. Increased water levels with pronounced stream inflows, cool conditions, open forest-steppe. F. Early glacial conditions, dry or temporarily flooded, landscape instability, cooling. Letters A–F correspond to Fig. 9.

juvenile *Pseudocandona* in sublevel II-4c of 12 II DB compared to the same sublevel in RP 13 II, however, hint at calmer conditions, at least during this phase, at site 12 II DB. Complementarily, the dominance of *Chara* cf. *hispida* in sequence 12 II DB (2009) clearly indicates greater water depth in comparison with RP 13 II. Lower abundances of the deep and stagnant water avoiding *Prionocypris zenkeri* further support both higher water levels and calmer conditions at site 12 II DB during deposition of sublevel II-4c.

In summary, species assemblages of both sites confirm inferred chemical lake water characteristics. Similar trends in the geochemical record, e.g. high carbonate contents especially in sublevel II-4c, giving evidence for an overall lake level rise at that time, are consistent with interpretations of Urban & Bigga (2015) and Kunz *et al.* (2017). However, contrasting the generally recorded greater disturbances and fluviatile influence at site 12 II DB, higher lake levels and a possibly more distal inflow are depicted in sub-sublevel II-4c1 of this sequence compared to RP 13 II.

Environmental development in the Reinsdorf sequence

Based on aquatic and terrestrial proxies, six main lakeshore development stages (Fig. 10A–F) are defined for the Reinsdorf sequence by Reference Profile 13 II (2003). Aquatic microfossils along with palynological results support repeated lake level variations (e.g. Mania 2007a; Urban 2007; Lang *et al.* 2012) and consequently climate-driven changes from aquatic to more terrestrial habitats at the study site. Aquatic microfossil assemblages and vegetation development (Figs 6, 8, 9) jointly allow for a refined reconstruction of environmental changes and their impact on the palaeolake ecosystem during the interglacial–glacial transition.

The Reinsdorf interglacial temperature maximum and beginning of cooler conditions. – The lowermost levels of RP 13 II represent the interglacial temperature maximum and terminal phase, showing a mid- to late interglacial vegetation succession reconstructed from five local pollen assemblage zones (LPAZ R1–R4/5, Fig. 6; Urban 1995, 2007; Urban & Bigga 2015).

Lack of aquatic microfossils in the lowermost part of RP 13 II, except for low abundances of ostracods in the upper part of sub-sublevel 13 II-2c4 (Fig. 8), suggests that the site was probably only temporarily covered by very shallow waters (Fig. 10A). This is consistent with the documented forest mire development (Urban 1995) as well as 3D subsurface modelling and shear wave seismics that suggest a lake level lowstand for 13 II-1a (Lang *et al.* 2012).

Steppe environment with increasing lake levels and habitat instability. – The continuous presence of a diverse ostracod fauna as well as occurrences of *Chara* cf. *vulgaris* remains in calcareous muds rich in mollusc shells document submerged conditions (Fig. 10B; OAZ1, Fig. 2). Increasing lake levels promoted development of a permanent water body with rich aquatic fauna and flora during deposition of sub-sublevels 13 II-2c3–II-2c1 (Fig. 10B).

In general, the ostracod assemblage is shaped by littoral species, which prefer shallow water. Mostly mesorheophilic or rheoeuryplastic ostracod taxa and the high OTI values (Fig. 2) suggest increased turbulent stream inflow from the Elm, consistent with Lang *et al.* (2015) and likely associated with reduced vegetation cover in the catchment. The zonal vegetation during this depositional period was characterized by high numbers of Poaceae, *Artemisia* and other terrestrial herbs. Among the tree and shrub pollen, *Betula*, *Juniperus* and *Larix* point to open landscape conditions and increasing dryness facilitating erosion (Fig. 6).

Diatoms were first observed in sub-sublevel 13 II-2c1 (Fig. 5). Dominating small tychoplanktonic fragilarioid diatom taxa (e.g. *Pseudostaurosira brevistriata*, *Staurosira venter*) are still indicative of a shallow lake (Bradbury 1988; Schmidt *et al.* 2004). Small *Fragilaria s.l.* are considered pioneer species occurring after disturbance events with erosion (Hickman & Reasoner 1994, 1998), and environmental instability is proposed to stimulate mass development (Denys 1990). Their fast reproduction rate and broad tolerances make them highly competitive in unstable, changing habitats (Hickman & Reasoner 1998; Lotter & Bigler 2000; Weckström & Juggins 2005). Mass occurrence of these taxa is also proposed to be associated with long periods of ice cover (Lotter & Bigler 2000). Cooler climates compared to the preceding thermal maximum of the Reinsdorf sequence, at least during winter, might have led to reduced evapotranspiration and consequently higher lake levels.

Change to a boreal forest-steppe with more stable aquatic lake-shore habitats and subsequent lake level drop. – Following the lake level increase indicated by sub-sublevels 13 II-2c3–II-2c1, sediments document progressive silting up of the site and deposition of silty organic muds with peaty layers (II-2b 2a(b)) (Table S1), which did not preserve ostracod shells (Fig. 10C, D).

Palynological and sedimentological evidence as well as plant macro-remains point to repeated dry-wet conditions changing from local swamps to areas of open water and back, beginning in the uppermost part of sub-sublevel 13 II-2c1 up to II-4e1 (LPAZ RP2a/b, RP3). A *Pinus* and *Betula* dominated boreal forest-steppe with *Salix*, *Populus* and *Juniperus* occurring more locally and *Picea* and *Larix* growing on drier stands are indicative of a longer cool-temperate dry period, which follows the cool and dry steppe phase of RP1 (Fig. 6).

A stable and productive aquatic ecosystem with diverse microhabitats is suggested by the highest ostracod concentration of the entire sequence and a high diversity (Fig. 2) in the lower part of level 13 II-3. While the diatom assemblages in the lowermost section are still dominated by disturbance indicating tychoplanktonic small *Fragilaria s.l.*, a distinctive shift to benthic diatom species, occurring in sublevels 13 II-3c/3b2 (beginning of DAZ2a) and prevailing up to sub-sublevel 13 II-4e3 (DAZ2b), supports more stable conditions (Fig. 5). PCA component 1 of diatom data further emphasizes this development by changing from negative to positive values. The reduction in small fragilarioid diatoms might additionally be related to shorter periods of ice cover on the lake, which fits the interpreted increased temperatures during a cool-temperate dry period based on palynological data.

A marked increase in TOC and TN contents (Fig. 8), especially between sublevels 13 II-3c/3b2 and II-4h1, indicates a change towards a more productive system or reduced input of minerogenic matter (Enters *et al.* 2006). The frequent occurrence of the fish species *Carassius carassius* starting in level II-3 rather suggests eutrophication took place (Böhme 2015). High C/N ratios (17–19), however, show a significant contribution of terrestrially derived organic matter (Meyers 1994).

A decrease in spring and flowing water-associated ostracod species (e.g. *Prionocypris zenkeri*) marks sublevels 13 II-3a–II-4e3 (OAZ2a/2b). Oligorheophilic species (e.g. *Pseudocandona compressa*, *Candona weltneri*) increase in abundance, the OTI reaches its lowest values of the whole sequence and PCA component 2 of ostracod data, mainly separating calm and more turbulence indicating species, shows a shift towards more positive values (Figs 7, 8). An increase in vegetation cover along the lake shore and accompanied reduced surface spring water discharge possibly explain the development towards a less turbulent environment.

Concurrently, ostracod-based reconstructed salinities show a maximum within the β-oligohaline salinity range, i.e. >2 (psu) (OAZ2a/2b), thereby indicating brine influence under positive precipitation–evaporation balance during this phase. Especially OAZ2b shows a marked salt influence, probably driven by subrosion

related to fluctuations of the groundwater table. Generally increased soluble salt contents in organic-rich Reinsdorf deposits were associated with periods of higher groundwater levels (Urban & Bigga 2015).

The interjacent event layer (sub-sublevel 13 II-4h1) is characterized by a high number of broken ostracod valves, low microfossil concentrations and the one-time appearance of the diatom species *Navicula lacuum*, together with increasing occurrence of otherwise rare taxa. Moreover, higher amounts of reworked palynomorphs and suddenly increased abundances of Ericaceae are evident. High input of allochthonous material, possibly as a result of a major erosion event of older lake sediments at the lake shore, could have been caused by changing dry-wet conditions or a short-lived climatic oscillation leading to lake level variations.

After this event layer, a decline in abundances of the diatoms *Cocconeis* spp. and *Rhoicosphenia abbreviata* in favour of *Cymbopleura inaequalis*, as well as the return of charophyte gyrogonites, is suggestive of less eutrophic conditions in sublevels 13 II-4g–II-4e3 (DAZ2b) compared to sublevels 13 II-3c/3b2–II-4h2 (DAZ2a), although productivity is still high as suggested by TOC and TN contents.

Overall, the concomitant changes in ostracod and diatom assemblages reflect a decreased inflow of surface waters accompanied by turbulence and erosion. Surface inflows were probably hampered by a more extensive vegetation cover, whereas groundwater discharge into the lake increased. Aquatic vegetation could have developed extensively, and productivity was high (Fig. 10C).

The disappearance of diatoms and ostracods following the period of less disturbed aquatic conditions in OAZ2a/2b and DAZ2a/2b suggests a further lake level drop during the deposition of sub-sublevels 13 II-4e2 and II-4e1 (Fig. 10D). This drop is also supported by crumbly-structured, clayey-silty muds (Table S1), an increase of terrestrial herbs as well as of *Calluna* and other Ericales, and an almost entire lack of aquatic taxa, pointing to wet-dry conditions and strong desiccation processes (LPAZ RP3) (Fig. 6).

Repeated period of increased lake levels and transition into a glacial phase. – The reappearance of ostracods starting in sublevel II-4c suggests another increase in lake levels favouring development of diverse aquatic organisms (Figs 2, 10E). The charophyte assemblages indicate water depths of at least 50 cm for RP 13 II and probably more than 2 m at site 12 II DB. The ostracod *Limnocythere inopinata* appears for the first time with constantly higher abundances in RP 13 II. In a study about the ecology and distribution of living ostracod assemblages in a lake in central Italy, *L. inopinata* was dominant in slightly deeper water areas (around 150–210 cm), while *C. vidua* (OAZ1) was common in shallower waters (20–140 cm) (Marchegiano *et al.* 2017). Therefore, higher lake levels in OAZ3, in comparison with OAZ1, could explain the different assemblages. Flowing water and spring input indicating ostracod taxa occur again frequently and the OTI values point to increased turbulence.

Very low numbers of Pinus and high values of heliophilic terrestrial herbs, with *Betula* being a major component of the riparian vegetation, characterize this phase (pollen subzones LPAZ RP4a and LPAZ RP4b, sublevel 13 II-4c) and show opening of the landscape and development of a steppe ecosystem under a cool continental climate (Fig. 6).

Small fragilarioid diatoms are again abundant in the upper part of sublevel 13 II-4c (DAZ3), comparable to DAZ1 (Fig. 5), hinting at similar unstable conditions with possibly longer duration of lake ice cover. The microfossil records thereby show again a climatic oscillation with lake level rise, flooding and increased influence of stream activity originating from the Elm causing turbulence and erosion in a deltaic or alluvial system (Fig. 10E).

Termination of the Reinsdorf sequence. – Sub-sublevel II-4a1/b in sequence 12 II DB (2009), corresponding to the 'Spear Horizon' of site 13 II, is void of diatom, ostracod and charophyte remains. Nonetheless, macro-remains and pollen of aquatic taxa were found in RP 13 II, suggesting submerged conditions at least in the beginning of this phase (Fig. 10F; Urban & Bigga 2015). Pollen analyses show another relatively temperate phase reflected by a *Pinus* increase, a drop of *Betula*, very few *Salix*, *Alnus*, *Juniperus* and *Picea* pollen and very rare occurrences of *Larix* (LPAZ RP5, sublevels 13 II-4a to II-4b(c)).

The succeeding level II-5 is again void of aquatic microfossils and reworked palynomorphs increase in abundance. The zonal vegetation and climatic conditions can be described as a highly continental open forest-steppe environment transitioning into another steppe phase with increased occurrences of Poaceae and Cyperaceae and decreasing amounts of *Betula* and *Pinus* (Fig. 6, LPAZ RP6). We propose climatic deterioration characterized by cool climates, a lake level drop, progressive desiccation and landscape instability during deposition of the uppermost part of RP 13 II and termination of the Reinsdorf sequence (Fig. 10F).

Conclusions

Ostracods, diatoms and charophytes generally record shallow, alkaline lake waters with slightly increased salinities (β-oligohaline), meso-eutrophic conditions and rich aquatic vegetation during phases of higher lake levels. We suggest inflows from the Elm as the origin of the increased calcium concentrations, whereas the salinization can be connected to the salt wall. The new results thereby support and concretize previous interpretations of e.g. pollen, plant macro-remains, fish and

sedimentological investigations regarding lake level variations, increased nutrient levels and salinities. Overall, aquatic microfossil analyses provide more detailed information about lake-shore structures and water depths at sites 12 II DB and 13 II (RP), as well as quantitative salinity data.

This Reinsdorf succession is characterized by six major lake-shore development stages with highly variable lake levels, aquatic habitats and vegetation patterns (A–F). The Reinsdorf Interglacial is followed by drier and cooler forest-steppe and steppe phases that ultimately transform into a cold phase. Lake levels were low in the beginning of the Reinsdorf sequence, which was characterized by thermophile, deciduous dominated interglacial forests (A). Progressive forest opening and steppe development in the catchment during cooler climates led to enhanced surface runoff and deposition in a lake-shore environment influenced by small, turbulent streams with elevated lake levels (B). Development of boreal forest-steppes with increased vegetation cover during a climate oscillation in the central part of the sequence resulted in calmer, shallow water conditions with generally higher trophic levels (C). Concurrently, brine influence, probably driven by stronger subrosion activity, increased. Following temporary desiccation (D), landscape opening, increasing spring water input via surface streams, and consequently increasing lake levels, favoured again growth of aquatic organisms at the lake shore during a late, cooler steppe phase in the younger part of the sequence (E). Progressive climate cooling, resulting in landscape instability and low lake levels, during an early glacial phase ultimately terminates the Reinsdorf sequence (F).

Multi-proxy studies are especially suited for archives subjected to highly variable conditions and sedimentological changes. The Reinsdorf deposits represent complex palaeolake-shore records with repeated phases of lake level rise and fall leading to the alternating deposition of lake marls and peat, as well as temporary desiccation, affecting the preservation of diatoms and calcareous microfossil remains. Therefore, a combined interpretation of aquatic and terrestrial proxies is needed and provides detailed information about Middle Pleistocene environmental changes around 300 ka ago that shaped early human habitats in Schöningen during periods of repeated landscape instability and climate cooling.

Acknowledgements. – We would like to thank Nicholas Conard, Sabine Gaudzinski-Windheuser, Andreas Koutsodendris, Volker Mosbrugger, Jordi Serangeli, Thomas Terberger, Elaine Turner, Thijs van Kolfschoten and the excavation team for supporting the project. We thank the student assistants who helped with the laboratory work and Theresia Lauke and Sarah Teuber for preparing their bachelor theses within this project. We are thankful to Birgit Plessen and Sylvia Pinkerneil for processing the geochemistry samples at the GFZ German Research Centre for Geosciences. Many thanks also to Carlos Wetzel for taking SEM pictures of some diatoms for taxonomic clarification and Anja Schwarz, Sandra Böddeker and John Smol for their helpful comments. The authors wish to thank David Horne and an anonymous reviewer for their constructive comments, which helped to significantly improve the manuscript. This research is a contribution to the project 'Climate and Environmental Variability during the late Middle Pleistocene at the Palaeolithic Sites of Schöningen, Northern Germany', funded by Deutsche Forschungsgemeinschaft (DFG grant SCHW 671/22-1, UR 25/11-1; project number 350769604). Further funding was received from the Ministry of Science and Culture (Niedersächsisches Ministerium für Wissenschaft und Kultur), Hannover, Germany (PRO*Niedersachsen, project: 74ZN1230).

Author contributions. – AS and BU designed the project and acquired funding. BU provided the sample material. KJK performed part of the aquatic microfossil laboratory work, conducted data processing and overall multi-proxy data interpretation, provided most of the figures and took the lead in writing the manuscript. BU and MT were responsible for palynological investigations as well as statistical pollen analysis and wrote the related paragraphs of the manuscript. MT prepared one figure. ISM helped with charophyte gyrogonite identification and interpretation of results. PF contributed to ostracod identification, ostracod data analysis and manuscript writing. JP performed part of the ostracod and charophyte laboratory work. All co-authors contributed to the manuscript by proofreading and discussions, especially AS.

Data availability statement. – The data that support the findings of this study are available from the corresponding author upon reasonable request.

References

Battarbee, R. W. & Kneen, M. J. 1982: The use of electronically counted microspheres in absolute diatom analysis. *Limnology and Oceanography 27*, 184–188.

Bigga, G. 2018: *Die Pflanzen von Schöningen. Botanische Makroreste aus den mittelpleistozänen Ablagerungen und das Nutzungspotential einer interglazialen Paläoflora. Forschungen zur Urgeschichte im Tagebau von Schöningen, Band 3*. 304 pp. Verlag des Römisch-Germanischen Zentralmuseums, Mainz.

Böhme, G. 2015: Fische, Amphibien und Reptilien aus dem Mittelpleistozän (Reinsdorf-Interglazial) von Schöningen (II) bei Helmstedt (Niedersachsen). *In* Terberger, T. & Winghart, S. (eds.): *Die Geologie der paläolithischen Fundstellen von Schöningen. Forschungen zur Urgeschichte aus dem Tagebau Schöningen, Band 2*, 203–265. Verlag des Römisch-Germanischen Zentralmuseums, Mainz.

Böhner, U., Fricke, C., Mania, D. & Thieme, H. 2005: *Schöningen 13 II, Referenzprofil. Stand April 2005. Dokumentationsdatenbank*. Niedersächsisches Landesamt für Denkmalpflege, Hannover.

ter Braak, C. J. F. 1983: Principal Components Biplots and Alpha and Beta Diversity. *Ecology 64*, 454–462.

Bradbury, J. P. 1988: Diatom biostratigraphy and the paleolimnology of Clear Lake, Lake County, California. *Geological Society of America, Special Paper 214*, 97–129.

Brandes, C., Pollok, L., Schmidt, C., Wilde, V. & Winsemann, J. 2012: Basin modelling of a lignite-bearing salt rim syncline: insights into rim syncline evolution and salt diapirism in NW Germany. *Basin Research 24*, 699–716.

Bridgland, D. R., Harding, P., Allen, P., Candy, I., Cherry, C., Horne, D., Keen, D. H., Penkman, K. E. H., Preece, R. C., Rhodes, E. J., Scaife, R., Schreve, D. C., Schwenninger, J.-L., Slipper, I., Ward, G., White, M. J., White, T. S. & Whittaker, J. E. 2013: An enhanced record of MIS 9 environments and geochronology: data from the construction of the channel tunnel rail-link and other recent investigations at Purfleet, Essex, UK. *Proceedings of the Geologists' Association 124*, 417–476.

Conard, N. J., Serangeli, J., Böhner, U., Starkovich, B., Miller, C. E., Urban, B. & van Kolfschoten, T. 2015: Excavations at Schöningen and paradigm shifts in human evolution. *Journal of Human Evolution 89*, 1–17.

Corillion, R. 1957: *Les Charophycées de France et d' Europe occidentale (étude systématique, écologique, phytosociologique et phytogéographique)*. 499 pp. Imprimerie Bretonne, Rennes.

van Dam, H., Mertens, A. & Sinkeldam, J. 1994: A coded checklist and ecological indicator values of freshwater diatoms from the Netherlands. *Netherlands Journal of Aquatic Ecology 28*, 117–133.

Denys, L. 1990: Fragilaria blooms in the Holocene of western coastal plain of Belgia. *In* Simola, H. (ed.): *Proceedings of the 10th International Diatom Symposium*, 397–406. Koeltz Scientific Books, Königstein.

Détriché, S., Bréhéret, J.-G., Soulié-Märsche, I., Karrat, L. & Macaire, J.-J. 2009: Late Holocene water level fluctuations of Lake Afourgagh (Middle-Atlas Mountains, Morocco) inferred from charophyte remains. *Palaeogeography, Palaeoclimatology, Palaeoecology 283*, 134–147.

Enters, D., Lücke, A. & Zolitschka, B. 2006: Effects of land-use change on deposition and composition of organic matter in Frickenhauser See, northern Bavaria, Germany. *Science of the Total Environment 369*, 178–187.

Faegri, K. & Iversen, I. 1989: *Textbook of Pollen Analysis*. 4th revised edition by Faegri, K., Kaland, P. E. & Krzywinski, K. 328 pp. John Wiley and Sons, Chichester.

Flower, R. J. 1993: Diatom preservation: Experiments and observations on dissolution and breakage in modern and fossil material. *Hydrobiologia 269*/270, 473–484.

Frenzel, P., Keyser, D. & Viehberg, F. A. 2010: An illustrated key and (palaeo)ecological primer for Postglacial to Recent Ostracoda (Crustacea) of the Baltic Sea. *Boreas 39*, 567–575.

Fuhrmann, R. 2012: Atlas quartärer und rezenter Ostrakoden Mitteldeutschlands. *Altenburger Naturwissenschaftliche Forschungen 15*, 1–320.

García, A. 1994: Charophyta: their use in paleolimnology. *Journal of Paleolimnology 10*, 43–52.

García, A. & Chivas, A. 2006: Diversity and ecology of extant and Quaternary Australian charophytes (Charales). *Cryptogamie, Algologie 27*, 323–340.

Gasse, F., Fontes, J.-C., Plaziat, J. C., Carbonel, P., Kaczmarska, I., De Dekker, P., Soulié-Märsche, I., Callot, Y. & Dupeuble, P. A. 1987: Biological remains, geochemistry and stable isotopes for the reconstruction of environmental and hydrological changes in the Holocene lakes from North Sahara. *Palaeogeography, Palaeoclimatology, Palaeoecology 60*, 1–46.

Grimm, E. C. 1987: CONISS: a Fortran 77 program for stratigraphically constrained cluster analysis by the method of incremental sum of squares. *Computers & Geosciences 13*, 13–35.

Grimm, E. C. 1990: Tilia, Tiliagraph & Tiliaview. PC spreadsheet and graphics software for pollen data. Illinois State Museum, IL, USA. www.geo.arizona.edu/palynology/geos581/tiliaview.html (accessed 1.6.2012).

Hammer, Á., Harper, D. A. T. & Ryan, P. D. 2001: PAST: Paleontological statistics software package for education and data analysis. *Palaeontologia Electronica 4*, 9. http://palaeo-electronica.org/2001_1/past/issue1_01.htm

Heijnis, H. 1992: *Uranium/Thorium dating of Late Pleistocene peat deposits in N.W. Europe*. Ph.D. thesis, Proefschrift Rijksuniversiteit Groningen, 149 pp.

Hickman, M. & Reasoner, M. A. 1994: Diatom responses to late Quaternary vegetation and climate change and to deposition of two tephras in an alpine and a subalpine lake in Yoho National Park, British Columbia. *Journal of Paleolimnology 11*, 173–188.

Hickman, M. & Reasoner, M. A. 1998: Late Quaternary diatom response to vegetation and climate change in a subalpine lake in Banff National Park, Alberta. *Journal of Paleolimnology 20*, 253–265.

Hoelzmann, P., Schwalb, A., Roberts, N., Cooper, P. & Burgess, A. 2010: Hydrological response of an east-Saharan palaeolake (NW Sudan) to early-Holocene climate. *The Holocene 20*, 537–549.

Horne, D. J. & Martens, K. 1999: Geographical parthenogenesis in European non-marine ostracods: post-glacial invasion or Holocene stability? *Hydrobiologia 391*, 1–7.

Horne, D. J., Curry, B. B. & Mesquita-Joanes, F. 2012: Mutual climatic range methods for Quaternary ostracods. *In* Horne, D. J., Holmes, J. A., Rodriguez-Lazaro, J. & Viehberg, F. (eds.): *Ostracoda as Proxies for Quaternary Climate Change*, 65–84. *Developments in Quaternary Science 17*.

Jechorek, H. 2000: Die fossile Flora des Reinsdorf-Interglazials. Paläokarpologische Untersuchungen an mittelpleistozänen Ablagerungen im Braunkohlentagebau Schöningen. *Praehistoria Thuringica 4*, 7–17.

Juggins, S. 2007: *C2 User Guide. Software for Ecological and Palaeoecological Data Analysis and Visualization*. 73 pp. Newcastle University, Newcastle.

Julien, M.-A., Hardy, B., Stahlschmidt, M. C., Urban, B., Serangeli, J. & Conard, N. J. 2015: Characterizing the Lower Paleolithic bone industry from Schöningen 12 II: a multi-proxy study. *Journal of Human Evolution 89*, 264–286.

Kalbe, L. & Werner, H. 1974: Sediment des Kummerower Sees. Untersuchungen des Chemismus und der Diatomeenflora. *Internationale Revue der gesamten Hydrobiologie 56*, 755–782.

van Kolfschoten, T. 2014: The Palaeolithic locality Schöningen (Germany): a review of the mammalian record. *Quaternary International 326–327*, 469–480.

Korsch, H. 2016: Chara vulgaris. *In* Arbeitsgruppe Characeen Deutschlands (ed.): *Armleuchteralgen. Die Characeen Deutschlands*, 379–387. Springer Verlag, Heidelberg.

Krammer, K. & Lange-Bertalot, H. 1986: *Bacillariophyceae, Part 1. Naviculaceae*. 876 pp. Gustav Fischer Verlag, Stuttgart.

Krammer, K. & Lange-Bertalot, H. 1988: *Bacillariophyceae, Part 2. Bacillariaceae, Epithemiaceae, Surirellaceae*. 611 pp. Gustav Fischer Verlag, Stuttgart.

Krammer, K. & Lange-Bertalot, H. 1991a: *Bacillariophyceae, Part 3. Centrales, Fragilariaceae, Eunotiaceae*. 598 pp. Gustav Fischer Verlag, Stuttgart.

Krammer, K. & Lange-Bertalot, H. 1991b: *Bacillariophyceae, Part 4. Achnanthaceae*. 468 pp. Gustav Fischer Verlag, Stuttgart.

Kumke, T., Kienel, U., Weckström, J., Korhola, A. & Hubberten, H.-W. 2004: Inferred Holocene paleotemperatures from diatoms at Lake Lama, Central Siberia. *Arctic, Antarctic and Alpine Research 36*, 624–634.

Kunz, A., Urban, B. & Tsukamoto, S. 2017: Chronological investigations of Pleistocene interglacial, glacial and aeolian deposits from Schöningen (Germany) using post-IR IRSL dating and pollen analysis. *German Journal of Geology 168*, 81–104.

Lang, J. & Winsemann, J. 2012: The 12II outcrop section at Schöningen: sedimentary facies and depositional architecture. *In* Behre, K.-E. (ed.): *Die chronologische Einordnung der paläolithischen Fundstellen von Schöningen*, 39–59. Verlag des Römisch-Germanischen Zentralmuseums, Mainz.

Lang, J., Böhner, U., Polom, U., Serangeli, J. & Winsemann, J. 2015: The Middle Pleistocene tunnel valley at Schöningen as a Paleolithic archive. *Journal of Human Evolution 89*, 18–26.

Lang, J., Winsemann, J., Steinmetz, D., Polom, U., Pollok, L., Böhner, U., Serangeli, J., Brandes, C., Hampel, A. & Winghart, S. 2012: The Pleistocene of Schöningen, Germany: a complex tunnel valley fill revealed from 3D subsurface modelling and shear wave seismics. *Quaternary Science Reviews 39*, 86–105.

Langangen, A. 2007: *Charophytes of the Nordic Countries*. 101 pp. Saeculum, Oslo.

Lange-Bertalot, H., Hofmann, G., Werum, M. & Cantonati, M. 2017: *Freshwater Benthic Diatoms of Central Europe: Over 800 Common Species Used in Ecological Assessment*. 942 pp. Koeltz Botanical Books, Schmitten-Oberreifenberg.

Last, W. M. & Smol, J. P. 2001: *Tracking Environmental Change Using Lake Sediments Volume 2: Physical and Geochemical Methods*. 504 pp. Kluwer Academic Publishers, Dordrecht.

Lauer, T. & Weiss, M. 2018: Timing of the Saalian- and Elsterian glacial cycles and the implications for Middle – Pleistocene hominin presence in central Europe. *Scientific Reports 8*, 5111, https://doi.org/10.1038/s41598-018-23541-w.

Löffler, H. 1959: Zur Limnologie. Entomostraken- und Rotatorienfauna des Seewinkelgebietes (Burgenland, Österreich). *Sitzungsberichte*

Österreichische Akademie der Wissenschaften, Mathematisch-Naturwissenschaftliche Klasse I 168, 315–362.
Löffler, H. 1990: Paleolimnology of Neusiedlersee, Austria. I. The succession of ostracods. *Hydrobiologia 214*, 229–238.
Lord, A. R., Boomer, I., Brouwers, E. & Whittaker, J. E. 2012: Ostracod taxa as palaeoclimate indicators in the quaternary. *Developments in Quaternary Science 17*, 37–45.
Lotter, A. F. & Bigler, C. 2000: Do diatoms in the Swiss Alps reflect the length of ice-cover? *Aquatic Sciences 62*, 125–141.
Mania, D. 1995: Die geologischen Verhältnisse im Gebiet von Schöningen. *In* Thieme, H. & Maier, R. (eds.): *Archäologische Ausgrabungen im Braunkohlentagebau Schöningen*, 33–43. Verlag Hahnsche Buchhandlung, Hannover.
Mania, D. 1998: Zum Ablauf der Klimazyklen seit der Elstervereisung im Elbe-Saalegebiet. *Praehistoria Thuringica 2*, 5–21.
Mania, D. 2007a: Das Eiszeitalter und seine Spuren im Tagebau Schöningen. *In* Thieme, H. (ed.): *Die Schöninger Speere – Mensch und Jagd vor 400 000 Jahren*, 35–61. Theiss, Stuttgart.
Mania, D. 2007b: Die fossilen Weichtiere (Mollusken) aus den Beckensedimenten des Zyklus Schöningen II (Reinsdorf-Warmzeit). *In* Thieme, H. (ed.): *Die Schöninger Speere - Mensch und Jagd vor 400.000 Jahren*, 99–104. Theiss, Stuttgart.
Marchegiano, M., Gliozzi, E., Ceschin, S., Mazzini, I., Adatte, T., Mazza, R., Gliozzi, S. & Ariztegui, D. 2017: Ecology and distribution of living ostracod assemblages in a shallow endorheic lake: the example of the Lake Trasimeno (Umbria, central Italy). *Journal of Limnology 76*, 469–487.
Mazzini, I., Gliozzi, E., Rossetti, G. & Pieri, V. 2014: The *Ilyocypris* puzzle: a multidisciplinary approach to the study of phenotypic variability. *International Review of Hydrobiology 99*, 395–408.
McCormack, J., Viehberg, F., Akdemir, D., Immenhauser, A. & Kwiecien, O. 2019: Ostracods as ecological and isotopic indicators of lake water salinity changes: the Lake Van example. *Biogeosciences 16*, 2095–2114.
Meisch, C. 2000: *Freshwater Ostracoda of Western and Central Europe*. 522 pp. Spektrum Akademischer Verlag, Heidelberg.
Meyers, P. A. 1994: Preservation of elemental and isotopic source identification of sedimentary organic matter. *Chemical Geology 114*, 289–302.
Moore, P. D., Webb, J. A. & Collins, M. E. 1991: *Pollen Analysis*. 216 pp. Blackwell Scientific, Oxford.
Pérez, L., Lorenschat, J., Massaferro, J., Paillès, C., Sylvestre, F., Hollwedel, W., Brandorff, G. O., Brenner, M., Islebe, G., Lozano, M. S., Scharf, B. & Schwalb, A. 2013: Bioindicators of climate and trophic state in lowland and highland aquatic ecosystems of the Northern Neotropics. *Revista de Biologia Tropical 61*, 603–644.
Pichler, C. 1997: Die Characeenflora des Neufelder Sees (Burgenland). *Verhandlungen der Zoologisch-Botanischen Gesellschaft in Österreich 134*, 33–46.
Pint, A., Frenzel, P., Horne, D. J., Franke, J., Daniel, T., Burghardt, A., Funai, B., Lippold, K., Daut, G. & Wennrich, V. 2015: Ostracoda from inland waterbodies with saline influence in Central Germany: implications for palaeoenvironmental reconstruction. *Palaeogeography, Palaeoclimatology, Palaeoecology 419*, 37–46.
Pint, A., Schneider, H., Frenzel, P., Horne, D. J., Voigt, M. & Viehberg, F. 2017: Late Quaternary salinity variation in the Lake of Siebleben (Thuringia, Central Germany) – Methods of palaeoenvironmental analysis using Ostracoda and pollen. *The Holocene 27*, 526–540.
Reed, J. M., Mesquita-Joanes, F. & Griffiths, H. I. 2012: Multi-indicator conductivity transfer functions for Quaternary palaeoclimate reconstruction. *Journal of Paleolimnology 47*, 251–275.
Richter, D. & Krbetscheck, M. 2015: Luminescence dating of the Lower Palaeolithic occupation at Schöningen 13/I. *Journal of Human Evolution 89*, 46–56.
Ryves, D. B., Battarbee, R. W., Juggins, S., Fritz, S. C. & Anderson, N. J. 2006: Physical and chemical predictors of diatom dissolution in freshwater and saline lake sediments in North America and West Greenland. *Limnology and Oceanography 51*, 1355–1368.
Sanjuan, J., Vicente, A., Flor-Arnau, N., Monleón, T., Cambra, J. & Martín-Closas, C. 2017: Effects of light and temperature on *Chara vulgaris* (Charophyceae) gyrogonite productivity and polymorphism – palaeoenvironmental implications. *Phycologia 56*, 204–212.
Schmidt, R., Kamenik, C., Lange-Bertalot, H. & Klee, R. 2004: *Fragilaria* and *Staurosira* (Bacillariophyceae) from sediment surfaces of 40 lakes in the Austrian Alps in relation to environmental variables and their potential for palaeoclimatology. *Journal of Limnology 63*, 171–189.
Schubert, H., Blindow, I. & van de Weyer, K. 2016: *Chara hispida*. *In* Arbeitsgruppe Characeen Deutschlands (ed.): *Armleuchteralgen. Die Characeen Deutschlands*, 307–317. Springer Verlag, Heidelberg.
Serangeli, J., Böhner, U., Hassmann, H. & Conrad, N. J. 2012: Die pleistozänen Fundstellen in Schöningen – eine Einführung. *In* Behre, K.-E. (ed.): *Die chronologische Einordnung der paläolithischen Fundstellen von Schöningen*, 1–22. Verlag des Römisch-Germanischen Zentralmuseums, Mainz.
Serangeli, J., Böhner, U., van Kolfschoten, T. & Conard, N. J. 2015: Overview and new results from large-scale excavations in Schöningen. *Journal of Human Evolution 89*, 27–45.
Serangeli, J., Rodríguez-Álvarez, B., Tucci, M., Verheijen, I., Bigga, G., Böhner, U., Urban, B., van Kolfschoten, T. & Conard, N. J. 2018: The Project Schöningen from an ecological and cultural perspective. *In* Cole, J. (ed.): Coping with climate: the legacy of *Homo heidelbergensis. Quaternary Science Reviews 198*, 140–155.
Sierralta, M., Frechen, M. & Urban, B. 2012: ^{230}Th/U dating results from opencast mine Schöningen. *In* Behre, K.-E. (ed.): *Die chronologische Einordnung der paläolithischen Fundstellen von Schöningen*, 143–154. Verlag des Römisch-Germanischen Zentralmuseums, Mainz.
Smol, J. P. & Stoermer, E. F. 2010: *The Diatoms: Application for the Environmental and Earth Sciences*. 667 pp. Cambridge University Press, Cambridge.
Smol, J. P., Birks, H. J. B. & Last, W. M. 2001a: *Tracking Environmental Change Using Lake Sediments Volume 3: Terrestrial, Algal and Siliceous Indicators*. 371 pp. Kluwer Academic Publishers, Dordrecht.
Smol, J. P., Birks, H. J. B. & Last, W. M. 2001b: *Tracking Environmental Change Using Lake Sediments, Volume 4: Zoological Indicators*. 217 pp. Kluwer Academic Publishers, Dordrecht.
Soulié-Märsche, I. 1989: *Etude comparée de gyrogonites de Charophytes actuelles et fossiles et phylogénie des genres actuels* (Thèse-ès-Sciences, Université Montpellier, 1979, revised edition). 237 pp. Millau, Imprimerie des Tilleuls.
Soulié-Märsche, I. 1991: Charophytes as lacustrine biomarkers during the Quaternary in North Africa. *Journal of African Earth Sciences 12*, 341–351.
Soulié-Märsche, I., Benkaddour, A., Elkhiati, N., Gemayel, P. & Ramdani, M. 2008: Charophytes, indicateurs de paléo-bathymétrie du lac Tigalmamine (Moyen Atlas, Maroc). *Geobios 41*, 435–444.
Soulié-Märsche, I., Bieda, S., Lafond, R., Maley, J., M'Baitoudji, M., Vincent, P. M. & Faure, H. 2010: Charophytes as bio-indicators for lake-level highstand at "Trou au Natron", Tibesti Chad, during the Late Pleistocene. *Global and Planetary Change 7*, 334–340.
Soulié-Märsche, I. & García, A. 2015: Gyrogonites and oospores, complementary viewpoints to improve the study of the charophytes (Charales). *Aquatic Botany 120*, 7–17.
Thieme, H. 1997: Lower Palaeolithic hunting spears from Germany. *Nature 385*, 807–810.
Thieme, H. 1999: Altpaläolithische Holzgeräte aus Schöningen, Lkr. Helmstedt. Bedeutsame Funde zur Kulturentwicklung des frühen Menschen. *Germania 77*, 451–487.
Thieme, H. 2007: *Die Schöninger Speere – Mensch und Jagd vor 400 000 Jahren*. 248 pp. Theiss, Stuttgart.
Tucci, M., Krahn, K. J., Richter, D., van Kolfschoten, T., Rodríguez Álvarez, B., Verheijen, I., Serangeli, J., Lehmann, J., Degering, D., Schwalb, A. & Urban, B. 2021: Evidence for the age and timing of environmental change associated with a Lower Palaeolithic site within the Middle Pleistocene Reinsdorf sequence of the Schöningen coal mine, Germany. *Palaeogeography, Palaeoclimatology, Palaeoecology 569*, 110309, https://doi.org/10.1016/j.palaeo.2021.110309.
Urban, B. 1995: Palynological evidence of younger Middle Pleistocene Interglacials (Holsteinian, Reinsdorf and Schöningen) in the Schöningen open cast lignite mine (eastern Lower Saxony, Germany). *Mededelingen Rijks Geologische Dienst 52*, 175–185.

Urban, B. 2007: Interglacial pollen records from Schöningen, north Germany. *In* Sirocko, F., Claussen, M., Sànchez Goni, M. F. & Litt, T. (eds.): *The Climate of Past Interglacials*, 417–444. Elsevier, Amsterdam.

Urban, B. & Bigga, G. 2015: Environmental reconstruction and biostratigraphy of late Middle Pleistocene lakeshore deposits at Schöningen. *Journal of Human Evolution 89*, 57–70.

Urban, B. & Sierralta, M. 2012: New palynological evidence and correlation of Early Palaeolithic sites Schöningen 12 B and 13 II, Schöningen open lignite mine. *In* Behre, K.-E. (ed.): *Die chronologische Einordnung der paläolithischen Fundstellen von Schöningen*, 77–96. Verlag des Römisch-Germanischen Zentralmuseums, Mainz.

Urban, B., Elsner, H., Hölzer, A., Mania, D. & Albrecht, B. 1991b: Eine eem- und frühweichselzeitliche Abfolge im Tagebau Schöningen, Landkreis Helmstedt. *Eiszeitalter und Gegenwart 41*, 85–99.

Urban, B., Lenhard, R., Mania, D. & Albrecht, B. 1991a: Mittelpleistozän im Tagebau Schöningen, Landkreis Helmstedt. *Zeitschrift der Deutschen Geologischen Gesellschaft 142*, 351–372.

Urban, B., Sierralta, M. & Frechen, M. 2011: New evidence for vegetation development and timing of Upper Middle Pleistocene interglacials in Northern Germany and tentative correlations. *Quaternary International 241*, 125–142.

Urban, B., Thieme, H. & Elsner, H. 1988: Biostratigraphische, quartärgeologische und urgeschichtliche Befunde aus dem Tagebau "Schöningen", Landkreis Helmstedt. *Zeitschrift der Deutschen Geologischen Gesellschaft 139*, 123–154.

Weckström, K. & Juggins, S. 2005: Coastal diatom-environment relationships from the Gulf of Finland, Baltic Sea. *Journal of Phycology 42*, 21–35.

van de Weyer, K. & Doege, A. 2016: *Chara globularis. In* Arbeitsgruppe Characeen Deutschlands (ed.): *Armleuchteralgen. Die Characeen Deutschlands*, 300–307. Springer Verlag, Heidelberg.

Wrozyna, C., Frenzel, P., Steeb, P., Zhu, L. P. & Schwalb, A. 2009: Recent lacustrine Ostracoda and a first transfer function for palaeowater depth estimation in Nam Co, southern Tibetan Plateau. *Revista Española de Micropaleontología 41*, 1–20.

Supporting Information

Additional Supporting Information may be found in the online version of this article at http://www.boreas.dk.

Table S1. Lithological description of Reference Profile Schöningen 13 II (2003) with pictures of the five profiles in stratigraphical order, elevation (m a.s.l.), level, square, sedimentological description and local pollen assemblage zones (LPAZ) (modified from Urban & Bigga 2015).

Table S2. Lithological description of sequence 12 II DB (2009) at plateau 4 showing four profile coordinates in stratigraphical order, level, sample ID (DBG only geochemical analysis), elevation (m a.s.l.), sedimentological description and local pollen assemblage zones (LPAZ) (modified from Kunz *et al.* 2017).